RSC Advances

ROYAL SOCIETY OF CHEMISTRY

www.rsc.org/advances

Mixed-ligand copper(II)-phenolate complexes: structure and studies on DNA/protein binding profile, DNA cleavage, molecular docking and cytotoxicity

Sellamuthu Kathiresan[a], Subramanian Mugesh[b], Maruthamuthu Murugan[b], Feroze Ahamed[b] and Jamespandi Annaraj[a]*

Abstract

Copper(II) complexes with simple and mixed ligands are constructed as, $[Cu(L)(ClO_4)]$ (**1**), $[Cu(L)(diimine)]ClO_4$ (**2**-**4**), [where L is 4-chloro-2-((2-(phenylthio)phenylimino)methyl)phenol and diimine is 1,10-phenanthroline (phen, **2**), 2,2'-bipyridine (bpy, **3**) and 4,4'-dimethyl-2,2'-bipyridyl (dmbpy, **4**)] were synthesized and characterized by elemental analysis, UV-vis, FT-IR, electrospray ionization-mass spectrometry (ESI-MS) and electrochemical studies. Especially, complex **4** was structurally characterized using single X-ray crystallographic technique. It is observed that it has slightly distorted square planar geometry. Their varying interactions with herring sperm DNA (HS-DNA) was explored in detail using various spectral and electrochemical methods to gain some insight into the structure-activity relationship. The obtained results revealed that complexes **1, 3** and **4** could interact with HS-DNA *via* partial intercalation mode whereas, complex **2** was found to be deep stacking between the base-pairs with the binding constant of 10^4 M^{-1} due to its enhanced planarity and **4** was involved in a hydrophobic interaction with DNA. These experimental observations were found to be near close to the theoretical observations, investigated through molecular docking technique. The interaction of these synthesized Cu(II) complexes with bovine serum albumin (BSA) was also evaluated using absorption and fluorescence techniques, which provided a static quenching mechanism between them. Additionally, the DNA cleavage by the complexes followed by electrophoretic spectrometric technique and the results showed that these complexes exhibited significant cleavage in the presence of reducing agent (ascorbic acid). The *in vitro* cytotoxicity of these Cu(II) complexes was carried out in two different human tumour cell lines, A549 and Huh7. Further molecular docking technique was also used to evaluate and understand the interaction modes of the complexes toward the molecular target DNA. All the *in vitro* pharmacological evaluation observations clearly indicated their better DNA binding/cleaving and protein binding properties though the S-donor atom did not coordinated with the central copper in their mixed complexes.

[a]Department of Materials Science, School of Chemistry, Madurai Kamaraj University, Madurai 625021, Tamil Nadu, India. E-mail address: annaraj.chem@mkuniversity.org
[b]Department of Microbial Technology, School of Biological Sciences, Madurai Kamaraj University, Madurai-625 021, Tamil Nadu, India

Electronic supplementary information (ESI) available: Fig. ^{1}H NMR, ^{13}C NMR, UV-vis, ESI-MS, CV and DPV of the ligand and complexes **1**–**4**. CCDC 1401459 for [Cu(L)(dmbpy)]ClO_4 **(4)**. For ESI and crystallographic data in CIF or other electronic format see DOI:

1. Introduction

Transition metal complexes play a vital role in nucleic acid chemistry due to their diverse applications such as sequence specific binding, structural probes and therapeutic agents, even though many drug molecules are organic in nature.[1-5] Cisplatin, a well-known metallo-drug for cancer, despite its wide applications as a chemotherapeutic agent, it exhibits several side effects, such as nausea, kidney and liver failure, typical of heavy metal toxicity.[6,7] Therefore, the researchers wish to found better alternative candidates of non-platinum based metal complexes such as copper, cobalt, nickel, zinc, ruthenium and iron, since they have very lower side effects.[8] DNA and proteins are the major cellular targets for cytotoxicity because of this interactions with small molecules, leads DNA damage in the cancer cells by blocking their uncontrolled division and resulting in cell death.[9–13] Currently, inorganic metal complexes have been successfully used as drugs in the treatment of many cancers.[14] Copper(II) complexes are considered and proposed as the better candidates for cancer therapy, since they exhibited a significant role in biological systems with no or negligible side effects.[15-17] Therefore much attention has been given to non-platinum based metal complexes that can interact with DNA and also due to their antioxidant properties. Similarly, proteins have also attracted the recent research community as a prime molecular target.[18] Nowadays interaction between proteins and metal complexes become key in the search of new drug molecules.[19,20] Since, the serum albumins such as, bovine serum albumin (BSA) is the most essential protein available in plasma that carries several endo and exogenous compounds. It is most crucial to explore the drug-protein interactions as most of the drugs bound to serum albumins are usually transported as a protein complex.[21,22]

Coordination chemistry of copper complexes of Schiff's base ligands with ONS and NO chromospheres are interesting due to their structural, spectral, and redox properties. Since the

complexes constructed with sulfur atom, their medicinal applications may anticipated to mimic the functional properties of sulfur-containing proteins.[23] It is well known that sulfur is an important constituent of biomolecules and plays a vital role in biological systems.[24] Recently, it has been reported that some Cu(II) complexes exhibited strong DNA interactions and induced apoptosis in

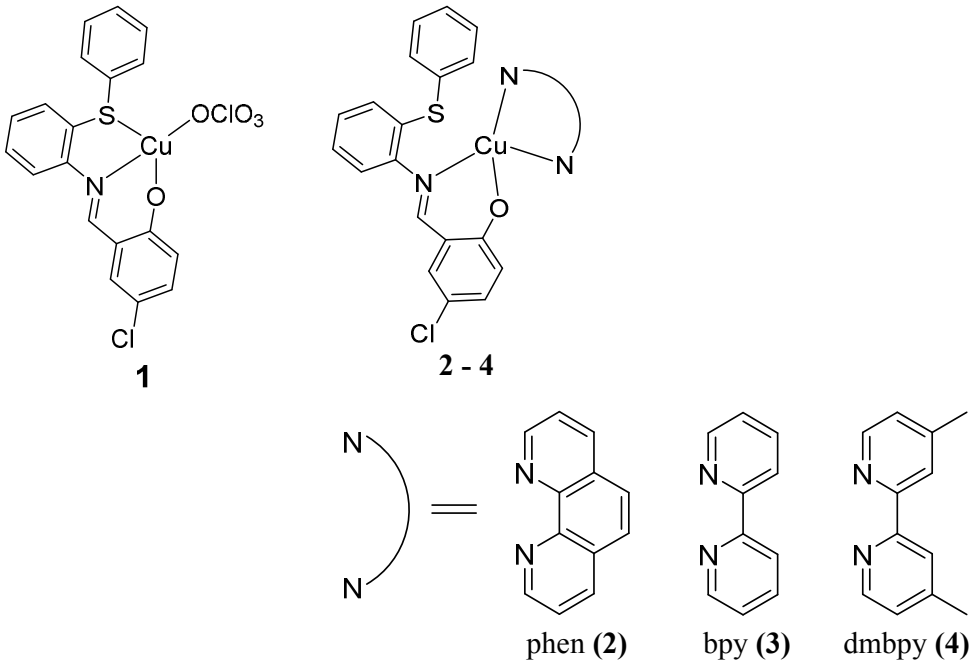

Scheme 1: Chemical structures of copper(II) complexes with diimine co-ligands.

cancer cells.[25-28] Therefore, the increasing importance of such sulfur containing copper(II) complexes also motivated us to propose some Cu(II) complexes with co-ligands[29] in order to evaluate their biological applications. In this article, we synthesized some copper(II) complexes, $[Cu(L)(ClO_4)]$ (**1**) of simple Schiff's base ligand, where L is the 4-chloro-2-((2-(phenylthio)phenylimino)methyl)phenol and a serious of mixed ligands of the type $[Cu(L)(diimine)]ClO_4$ where diimine = 1,10 phenanthroline (phen) (**2**), 2,2'-bipyridine (bpy) (**3**), 4,4'-dimethyl-2,2'-bipyridyl (dmbpy) (**4**) and explored their DNA/protein binding and DNA cleaving abilities depends upon the structure and number/size of the aromatic rings present in the Cu(II) complexes. Unfortunately, the sulfur atom did not coordinated to the central Cu(II) ion in the presence of co-ligands (phen, bpy and dmbpy), therefore it could not be comparable with previously reported sulfur containing copper complexes[23-29] of biomimetic copper enzyme models, even though this manuscript aimed to deals on their possible biological applications. The diimines such as bpy can able to recognize and binding to DNA, thus the introduction of methyl groups on the 4,4'-position of the bpy ring, (e.g., dmbpy)

would provide a hydrophobic recognition element.[30] Furthermore the *in vitro* cytotoxicity of the copper(II) complexes against lung (A549) and liver (Huh7) cancer cell lines were also investigated.

2. Experimental

***Caution**:* Perchlorate salts of metal complexes are potentially explosive and therefore should be prepared in a small quantity.

2.1 Materials

The AR grade commercially available reagents and chemicals were obtained from (Sigma-Aldrich, India, S.D Fine chemicals, India, CDH, India, Fluka, India) respectively. Copper(II) perchlorate hexahydrate, 5-chloro salicyaldehyde, ethidium bromide (EtBr), 4,4'-dimethyl-2,2'-bipyridyl (Aldrich), 1,10-phenanthroline (CDH), 2,2'-bipyridine (S.D Fine), 2-(phenylthio)aniline (Fluka), Herring sperm DNA (SRL), Tris (hydroxymethyl)aminomethane-HCl (Tris-HCl) (SRL) and sodium chloride (SRL), supercoiled pUC18 plasmid DNA (Merck), bovine serum albumin (BSA) (Himedia) were purchased from the respective agencies which are mentioned in the within-bracket and used without further purification. Spectroscopic grade ethanol was purchased from Merck and was used without further purification. Dimethyl sulfoxide (DMSO) and ethylenediaminetetraaceticacid (EDTA) were purchased from Sigma-Aldrich. Tetrabutylammonium perchlorate (TBAP) was purchased from Fluka. A549 (lung cancer cells) and Huh7 (liver cancer cells) were purchased from national centre for cell sciences. DMEM-F12 Ham, Fetal Bovine Serum (FBS), antibiotics, and other growth supplements were purchased from Himedia Chemicals, India. Reagent-grade 3-(4,5-dimethylthiazol-2-yl)-2,5-diphenyltetrazolium bromide (MTT) was obtained from Calbiochem.

2.2 Methods and instrumentations

^{1}H and ^{13}C NMR spectra were recorded on a high resolution Bruker 300 MHz spectrometer in $CDCl_3$ solution using TMS as the internal standard. Chemical shifts (ppm) were reported relative to tetramethylsilane (Me_4Si). Melting points were determined on a Sigma capillary melting point apparatus. The elemental analyses were determined using a Vario III CHNS analyzer. FT-IR spectra of the ligand and complexes were recorded using KBr pellets on a JASCO FT-IR 410 double beam infrared spectrophotometer in the range of 4000-400 cm^{-1}. Electrospray Ionization Mass Spectrometry (ESI-MS) analysis was performed in the positive ion mode on a liquid chromatography-ion trap mass spectrometer (LCQ Fleet, Thermo Fisher Instruments Limited, USA). Electronic absorption spectra were recorded using an Agilent 8453 UV-vis Spectrophotometer in the

range 190–1100 nm. Emission spectra were recorded using Agilent Cary Eclipse fluorescence spectrophotometer. Circular dichroism spectroscopy was performed with JASCO J-810 Spectropolarimeter, the spectra of the DNA solutions with addition of complex at 25 ^{o}C were recorded using a quartz cuvette of 1 cm optical path length. Cyclic voltammetry and differential pulse voltammetry measurements for these complexes were carried out using a Model CH 680 electrochemical analyzer with three electrode system of a glassy carbon as the working (GCE), Ag/AgCl reference and a platinum wire as the auxiliary electrodes respectively under N_2 atm. Electrochemical measurements were performed in CH_3CN solutions with 0.1 M TBAP as the supporting electrolyte at room temperature. The surface of GC electrode was cleaned with alumina powder before every measurement. Tris-HCl buffer (pH 7.1) was used as a supporting electrolyte during the investigation of interaction between complexes and DNA, the solutions were deoxygenated by purging with N_2 for 15 min prior to every measurement.

2.3 Synthesis of ligand L and corresponding Cu(II) complexes

2.3.1 Synthesis of 4-chloro-2-((2-(phenylthio)phenylimino)methyl)phenol (L)

2-(Phenylthio)aniline (0.1286 g, 1 mmol) was added dropwise to an ethanol solution of 5-cholro 2-hydroxy benzaldehyde (0.1 g, 1 mmol) under constant stirring. The reaction mixture was then refluxed for further 2 h and then kept aside for six hours at room temperature. The obtained yellow crystalline solid as product that formed was filtered off, washed several times with cold ethanol and dried in a *vacuo* (purity was checked by TLC).

Yield: 90%; color: yellow; MP: 98–102 ^{o}C; ^{1}H NMR (300 MHz, $CDCl_3$) δ 13.10 (1H, s, –OH), 8.51 (1H, s, CH=N), 7.57 – 6.97 (12H, m, Ar–H). ^{13}C NMR (75 MHz, $CDCl_3$) δ 160.88, 159.53, 146.41, 133.58, 132.90, 132.60, 132.38, 131.03, 130.42, 129.13, 128.77, 127.56, 127.44, 126.55, 123.39, 119.76, 118.79, 117.83. IR: (KBr pellet, cm^{-1}): 1618 (s), 1558 (m), 1465 (s), 736 (s). UV-vis (MeOH, λ_{max} (nm)): 270, 356. ESI-MS (MeOH): Found *m/z* = 340.09 $(M + H)^+$ (calcd *m/z* = 339.05).

2.3.2 Synthesis of [Cu(L)(ClO_4)] (1)

Methanolic solutions of copper(II) perchlorate hexahydrate (0.109 g, 1 mmol) and L (0.100 g, 1 mmol) was refluxed for 1 h. The obtained green colored precipitate was separated, washed with cold methanol/diethyl ether and dried in *vacuo* at RT.

Yield: 82%; color: light green; MP: 145 ^{o}C; Anal. Calcd for. $C_{19}H_{13}Cl_2CuNO_5S$: C, 45.48; H, 2.61; N, 2.79; Found: C, 45.64; H, 2.53; N, 2.68; IR: (KBr pellet, cm^{-1}): 1606 (s), 1556 (m), 1467 (s),

753 (s). UV-vis (MeOH, λ_{max} (nm)): 236, 280, 407 and 682 (d-d transition). ESI-MS (MeOH): Found *m/z* = 400.94 $[M - ClO_4]^+$ (calcd *m/z* = 499.05).

2.3.3 Synthesis of $[Cu(L)(phen)]ClO_4$ (2)

Methanolic solutions of copper(II) perchlorate hexahydrate (0.109 g, 1 mmol) and L (0.100 g, 1 mmol) was refluxed for 1 h, 1 mmol of phen (0.058 g) was added to the above reaction mixture and the reflection was continued for further 1 h. The obtained complex **2** as green colored precipitate was separated, washed with cold methanol/diethyl ether and dried in *vacuo* at RT.

Yield: 80%; color: dark green; MP: 160 ^oC; Anal. Calcd for. $C_{31}H_{21}Cl_2CuN_3O_5S$: C, 63.91; H, 3.63; N, 7.21; Found: C, 63.98; H, 3.57; N, 7.08; IR: (KBr pellet, cm^{-1}): 3419 (br), 1606 (s), 1516 (m), 1430 (s), 736 (s). UV-vis (MeOH, λ_{max} (nm)): 228, 268, 423 and 616 (d-d transition). ESI-MS (MeOH): Found *m/z* =581.03 $[Cu(L)(phen)]^+$ (calcd *m/z* = 581.04).

2.3.4 Synthesis of $[Cu(L)(bpy)]ClO_4$ (3)

Comp1ex **3** was prepared as the above mentioned procedure, using 1 mmol of bpy (0.058 g) instead of phen.

Yield: 76%; color: green; MP: 245–250 ^oC; Anal. Calcd for. $C_{29}H_{21}Cl_2CuN_3O_5S$: C, 62.36; H, 3.79; N, 7.52; Found: C, 62.14; H, 3.62; N, 7.37; IR: (KBr pellet, cm^{-1}): 3372 (br), 1604 (s), 1477 (m), 1444 (s), 732 (s). UV-vis (MeOH, λ_{max} (nm)): 237, 301, 411 and 608 (d-d transition). ESI-MS (MeOH): Found *m/z* = 558.88 $[Cu(L)(bpy)]^+$ (calcd *m/z* =557.04).

2.3.5 Synthesis of $[Cu(L)(dmbpy)]ClO_4$ (4)

Comp1ex **4** also was prepared as the above mentioned procedure, using 1 mmol of dmbpy (0.054 g) instead of phen or bpy. The obtained green colored single crystals which is suitable for X-ray diffraction was separated, washed with cold methanol/diethyl ether and dried in *vacuo* at RT

Yield: 85%; color: dark green; MP: 235–240 ^oC; Anal. Calcd for. $C_{31}H_{25}Cl_2CuN_3O_5S$: C, 63.47; H, 4.30; N, 7.16; Found: C, 63.26; H, 4.18; N, 7.08; IR: (KBr pellet, cm^{-1}): 3475 (br), 1608 (s), 1519 (m), 1450 (m), 734 (s). UV-vis (MeOH, λ_{max} (nm)): 245, 292, 411 and 653 (d-d transition). ESI-MS (MeOH): Found *m/z* = 584.96 $[Cu(L)(dmbpy)]^+$ (calcd *m/z* = 585.07).

2.4 Single crystal X-ray crystallography

Single crystal of complex $[Cu(L)(dmbpy)]ClO_4$ **(4)** was obtained by slow evaporation of methanol solution at room temperature. Single crystal X-ray diffraction data for complex **4** were

collected on a Bruker APEX2 CCD area-detector diffractometer at 293(2) K using a graphite monochromated Mo Kα radiation (λ= 0.71073 Å). The collected data were reduced by using the XCAD4 program.[31] The structure was solved by direct methods as implemented in SHELXS-97 program.[32] The position of all the non-hydrogen atoms were included in the full–matrix least squares refinement using SHELXL-97 program.[32] The molecular graphics were depicted by the program ORTEP-3 for windows.[33] The crystallographic data and structure refinement parameters are summarized in Table 1, and the selected bond distances, angles are listed in Table 2. Crystallographic data (excluding structure factors) for the structure reported have been deposited with the Cambridge Crystallographic Data Centre as supplementary CCDC deposition No. 1401459.

2.5 DNA interaction studies

2.5.1 Electronic absorption titration. Electronic absorption spectra were determined in the range of 300–600 nm by constant concentration of copper(II) complexes (100 μM) and varying the concentration of HS-DNA (0–50 μM). The stock solution of HS-DNA was prepared with a buffer (5 mM Tris-HCl/50 mM NaCl, pH 7.1) and stored at 4 ^{o}C for complete dissolution and used over not more than 4 days. The concentration of HS-DNA was determined by UV absorbance at 260 nm, taking 6600 M^{-1} cm^{-1} as the molar absorption coefficient.

2.5.2 Fluorescence spectroscopy. The competitive binding study was carried out by maintaining the [DNA]/[EtBr] ratio of 10:1, it was prepared by addition of EtBr (250 μL, 10^{-3} M) and DNA (1250 μL, 2 x 10^{-3} M) into Tris-HCl buffer solution at (25 mL, pH=7.1). Emission spectra were recorded in the region between 550–750 nm at room temperature with fixed excitation wavelength at 525 nm during the addition of increasing concentration of the synthesized complexes **1**–**4**. The fluorescence spectra of solutions containing EtBr-DNA bound mixture with various concentrations of **1**–**4** (0–150 μM) were taken.

2.5.3 Electrochemical methods. Cyclic and differential pulse voltammogram experiments were carried out with a three electrode apparatus using a Model CH 680 electrochemical analyzer. The complexes were dissolved in MeOH to the desired concentrations. All experiments were carried out between a fixed concentration of Cu(II) complexes and absence and presence of HS-DNA. The potential and current changes during the addition of increasing HS-DNA concentration were used to monitor in order to investigate the binding ability of the complexes with HS-DNA.

2.5.4 Circular dichroism (CD) spectroscopy. Circular dichroic spectra of DNA in the presence and absence of metal complexes [1/R= [Complex]/[DNA] (r = 0.2–1.0)] were recorded on a JASCO J-810 (163–900 nm) spectropolarimeter using a quartz cuvette with 1 cm optical path length. Each

sample was scanned in the range of 200–400 nm. Every CD spectrum was collected after averaging over at least four accumulations using a scan speed of 100 nm min^{-1} in one second time response from which the buffer background had been subtracted [DNA] =100 μM.

2.6 DNA cleavage studies

Cu(II) complexes were investigated for their DNA cleaving properties using agarose gel electrophoresis in the presence of 100 μM of ascorbic acid (H_2A).[34] Cu(II) complexes (in the range of 10–100 μM) were treated with plasmid pUC18 DNA (0.2 μg, ~30 μM base pairs). These samples (5 μL in Tris-buffer) were incubated at 37 ^oC for 1 h, to this solution a loading buffer (1 μL) consisting of 0.25% bromophenol blue and 30% glycerol were added. This mixture was brought to gel electrophoresis on 1% agarose in a 1× TAE buffer (40 mM Tris-acetate and 1 mM EDTA) at 50 V for 2 h. Pre-stained gel with ethidium bromide was photographed under UV light after electrophoresis. The cleaving properties were determined based on the ability of the Cu(II) complexes to convert the supercoiled form (Form I) into nicked circular form (Form II).[35]

2.7 Molecular docking studies

Molecular docking is an essential *in silico* computational tool for the rational design of novel chemotherapeutic drugs, which estimates the occurred non-covalent interactions between the drugs and the nucleic acids of DNA. A blind docking calculation for the complex and DNA was performed by the AutoDock (MGL Tools) package. Target molecule HS-DNA $d(ACCGACGTCGGT)_2$ structure was obtained from Protein Data Bank (PDB id: 423D).[36] The parameter values obtained from MGL (Molecular Graphics Laboratory) mailing lists forum (http://mgldev.scripps.edu)[37] were added to the Cu(II) complexes. X-ray crystal structure of Cu(II) complex **4** was converted as PDB format using Chem3D (Cambridge Soft).[38] Bound ligand ClO_4 coordinates from the complex **4** was removed and subsequently bound orders were checked to validate the docking protocol.[39] Complexes **1**, **2** and **3** were optimized at B3LYP/LANL2DZ level using G09W program then converted to PDB format using Chem3D (Cambridge Soft).[38] The docking calculated data of DNA and complexes were prepared using AutoDock Tools (ADT) and they were converted to PDBQT file. Grid boxes for Cu(II) complexes and DNA were constructed with 0.700 Å grid spacing and grid points in x×y×z directions, 64×114×62. Lamarckian genetic algorithm (LGA) has followed to perform docking calculations and for other parameters used as default. Visualization of the docked pose was done by PyMOL (The PyMOL Molecular Graphics System, Version 1.5.6) molecular graphics program.[40]

2.8 Protein binding studies

Protein binding study of Cu(II) complexes (**1**–**4**) with BSA was studied using fluorescence spectra of excitation 280 nm and emission 348 nm wavelengths respectively, corresponding to that of free bovine serum albumin (BSA). The excitation and emission slit widths and scan rates were constantly maintained for all the experiments. Stock solution of BSA was prepared in Tris-HCl buffer (pH = 7.1) and stored in the dark at 4 ^{o}C for further use. Concentrated stock solutions of test complexes were prepared by dissolving them in methanol and diluted suitably with Tris-HCl buffer to get required concentrations. BSA (2 mL, 1 μM) was titrated with the successive additions of complexes (10 μL, 10^{-3} M) using a micropipette. For UV-vis absorption experiment, the BSA (10 μM) was titrated with 5 μM concentration of the copper(II) complexes.

2.9 Cytotoxic studies

Copper(II) complexes were subjected to study the viability of human lung (A549) and liver (Huh7) cancer cells respectively by the well-known MTT assay method.[41] Lung adenocarcinoma cells (A549) and liver hepatocarcinoma cells (Huh7) were transferred into 96 well plates at a concentration of 1×10^{5} cells per well. Cu(II) complexes (1–50 μM) in DMSO were seeded in the well and incubated for 24 h with MTT [5 mg mL^{-1} phosphate buffer saline (PBS)] assay at 37 ^{o}C for 4 h. Their absorbance was measured at a wavelength of 570 nm and the percentage of cell viability was calculated by the following equation,

$$\frac{\text{Mean OD of the untreated cells (control)} - \text{mean OD of the treated cells}}{\text{Mean OD of the untreated cells (control)}} \times 100$$

3. Results and discussion

3.1 Physical properties of ligands and complexes

Ligand L was prepared by the reaction between 2-(phenylthio)aniline and 5-cholro-2-hydroxy benzaldehyde in ethanol. The obtained product was confirmed by ESI mass spectrometry and ^{1}H & ^{13}C NMR. The complexes were crystalline, non-hygroscopic solids, air-stable in both solution as well as solid states at room temperature and mostly soluble in common organic solvents. These complexes have been characterized by elemental analysis, ESI-MS, FT-IR, UV-vis spectral and electrochemical techniques. In addition, the structure of complex **4** was confirmed by single crystal X-ray crystallography.

3.2 Spectroscopic studies

A strong band for Schiff base ligand appeared in the 1618–1604 cm^{-1} region corresponding to υ(C=N) was underwent a coordination-induced shift to 1606 cm^{-1} for the complexes **1**–**4** which indicated that the coordination might be occurred through azomethine nitrogen of the ligands.[42] The band appeared at 736 cm^{-1} for υ(C-S) in the Schiff base was also significantly altered in complex **1** and appeared at 756 cm^{-1}, noticed that the coordination occurred between central Cu^{2+} ion and S atom of the ligand.[43] However, this band did not undergo any remarkable shift after complexation in complexes **2-4**, which clearly noticed that there is no bond formation occurred between copper centre and S donor present in the ligand.

Electronic spectra of all the complexes (**1**–**4)** were recorded in methanol, they showed three strong absorptions in the range of 423–228 nm. The absorbance appeared around 228–301 nm region have been assigned to the intra-ligand transitions and the lower energy absorptions perceived around 407–423 nm are assigned for the LMCT transitions.[44,45] Weak absorptions which observed in the range of 608–682 nm are assignable to their d-d transitions (Fig. S3).[46]

The ESI-MS spectra (in the positive-ion mode) for ligand and complexes **1**–**4** have been recorded in methanol. The ligand showed a peak at *m/z* 340.09 $[M + H]^+$ and complex **1** showed peak at 400.94 $[M – ClO_4]^+$. The mixed ligand complexes **2**, **3** and **4** were also showed their characteristic molecular ion peaks at *m/z* 581.03 $[Cu(L)(phen)]^+$ *m/z* 558.88 $[Cu(L)(bpy)]^+$ and *m/z* 584.96 $[Cu(L)(dmbpy)]^+$ respectively (Fig. S4-S8).

3.3 X-ray crystallography

The solid state X-ray molecular structure of complex, $[Cu(L)(dmbpy)]ClO_4$ (**4**) has been determined by single crystal X-ray diffraction study (Fig. 1) to predict the coordination mode of Schiff base ligand to the central copper and its stereochemistry. Suitable crystals of complex **4** were developed by slow evaporation of its methanolic solution, collected data and refinement parameters were summarized in Table 1, crystal data and selected interatomic bond lengths and angles were given in Table 2. The complex crystallizes as a triclinic crystal system with space group $P\bar{1}$. The copper atom has N_3O coordination through the phenolate oxygen atom, O5 and the imine nitrogen atoms (N1) of the primary ligand, remaining two corners were bonded with the two nitrogen atoms of co-ligand (N2 and N3, dmbpy). The obtained X-ray diffraction structure of complex **4** noticed that a slight distortion was occurred in its square planar geometry along with the angles of N(1)–Cu(1)–N(3) 161.79(11) to O(5)–Cu(1)–N(2) 163.64(11) from O(5)–Cu(1)–N(1) 92.07(11) to O(5)–Cu(1)–N(3) 89.83(11). The N(1)–Cu(1)–N(2) and N(3)–Cu(1)–N(2) bond angles of 101.04(11) and 80.78(11). However the sum of the angles in Cu(II) is very close to 360° indicating its planar

geometry. There is a significant bond distances occurred between metal centre and donor sites are Cu(1)–O(5) 1.879(2), Cu(1)–N(1) 1.984(3), Cu(1)–N(3) 1.999(3) and Cu(1)–N(2) 2.015(3) Å, which is similar to that found in Fig. 1. The dmbpy N atoms are slightly elongated from the M–N and M–O bond distances. The bond distances and bond angles are in good agreement for the observed slightly distorted square planar geometry of copper complexes with the previous reports.[47]

3.4 Electrochemistry

The cyclic voltammograms of all the copper complexes (**1**-**4**) were recorded in CH_3CN with glassy carbon electrode at a scan rate of 100 mV s^{-1} using 0.1 M tetrabutylammonium perchlorate (TBAP) as a supporting electrolyte. All the potentials were referenced with an Ag/AgCl electrode. All the complexes have shown a well-defined quasi-reversible redox couple. The cyclic voltammogram of complex **2** was illustrated in Fig. 2, and it showed a well-defined Cu^{II}/Cu^{I} quasi-reversible redox couple at 0.052 V. The i_{pa}/i_{pc} falls at ca. 0.91, clearly confirming one electron transfer in this redox process. Similarly quasi-reversible redox behaviour was observed for other complexes (Fig. S9). The redox potential of complex **2** was relatively higher than that of complexes **3** and **4**, which is due to the presence of phen moiety and it is attributed to the extension of the corresponding π framework around the metal centre.[48]

3.5 DNA binding studies

3.5.1 Electronic absorption titration

The changes occurred in the intra-ligand bands of **1**-**4** in 10% MeOH/5mM Tris-HCl/50 mM NaCl buffer at pH 7.1 were determined as a function of added DNA concentration. The electronic spectral technique is an effective tool to perceive the binding affinity between the Cu(II) complexes and DNA. Generally, hypochromism with or without red/blue shifts[49] are associated with the intercalative mode of binding nature due to the serious perturbation occurred on the sugar phosphate backbone by the deep penetration and stacking of the planar aromatic chromophore between the base pairs of DNA, whereas a non-intercalative/electrostatic interactions may show hyperchromism along with blue shift. The absorption spectra of the complexes at a constant concentration (100 μM) in the presence of different concentrations of HS-DNA to R= [DNA]/[complex]=(0–4) was given in Fig. 3. As shown in the figure, the increasing addition of DNA with complexes and decrease in molar absorptivity along with significant red shifts were observed for complexes **1**–**4**. These absorptivity changes are typical of a complex bound to DNA through stacking involving partial insertion of the aromatic chromophore of the diamine ligands in between the DNA base pairs depending upon their

chemical structure. The quantitative comparison of the DNA binding affinities of the complexes are obtaining the intrinsic binding constants K_b by using the equation.[50]

$$[DNA]/(\varepsilon_a-\varepsilon_f) = [DNA]/(\varepsilon_b-\varepsilon_f) + 1/K_b\ (\varepsilon_b-\varepsilon_f)$$

Where [DNA] is the concentration of DNA, ε_a is the apparent extinction coefficient obtained by calculating A_{obs}/[complex], ε_f and ε_b are the extinction coefficients of the complex in its free and bound forms respectively. It can be determined by screening the observed spectral changes (Fig. 3) on the intra-ligand band at the corresponding λ_{max} with the addition of increasing concentration of DNA. The intrinsic binding constant, K_b was obtained by the ratio of the slope to the y intercept by plotting $[DNA]/(\varepsilon_a - \varepsilon_f)$ *versus* [DNA], to monitor the magnitude of the binding strength. From the intrinsic binding constant values (Table 3), it is inferred that complex **2** exhibits efficient intercalative mode of binding than the other complexes and K_b values determined from these changes follow the order **2 > 4 > 3 > 1**, which is in conformity with the hypochromism observed in the spectra. Complex **3** showed a lower binding affinity than **2** and **4** due to the presence of non-planar bpy moiety, and it involved in a weaker electrostatic interaction with the negatively charged phosphate groups on the DNA backbone.[51] Additionally, the presence of electron donating methyl groups on the bpy ring would be expected to hinder even the partial insertion of the bpy ring leading to a lower DNA binding affinity for **4**. Though, a deep suppression of the intra-ligand band at 480 nm and observed higher K_b value than **3** and **1** suggesting a strong hydrophobic interaction occurred between the methyl groups of dmbpy ligand in **4** and the hydrophobic inner accessible in DNA.[52-54] The observed variable spectral changes between complex **3** and **2**, reveals that the decreasing planarity by the presence of bpy moiety leads partial intercalation or weaker electrostatic interaction with DNA surface. These spectral changes are useful features to optimize the recognition of metallo-drugs and DNA molecules.

3.5.2 Ethidium bromide displacement assay

In order to further understand the mode of interaction between these Cu(II) complexes and DNA,[55,56] ethidium bromide displacement experiments were carried out using fluorescent spectroscopy technique, since there is no fluorescence properties have been observed for the complexes alone or the accompany of HS-DNA at room temperature in solution. Generally, EtBr emits intense fluorescent light in the presence of DNA due to its strong intercalation between the adjacent DNA base pairs[57,58] If the metal complex or quencher intercalates into DNA, it leads to a significant decrease in the binding sites of DNA available for EtBr by quenching the intensity of the EtBr bound HS-DNA complex.[59,60] The extent of quenching in the fluorescence intensity of HS-

DNA-EtBr, reflects the extensive interaction of the copper complexes by replacing EtBr from the EtBr bound DNA takes place. The emission spectra of the DNA−EtBr system with the addition of increasing concentration of the Cu(II) complexes appeared at 603 nm are illustrated in Fig. 4. These observed decrease in the fluorescence intensity inferred that the EtBr molecules were displaced from their DNA binding sites and are replaced by the complexes under investigation. These observation occurred may be due to the intercalation/partial intercalation of the complexes **1**–**4** between the base pairs of HS-DNA, also it was explained by the Stern-Volmer equation.[61]

$$I_0/I = K_{sq}[Q] + 1$$

Where, I_o is the emission intensity in the absence of a quencher, I is the emission intensity in the presence of a quencher, K_{sq} is the quenching constant, and [Q] is the concentration of quencher. The K_{sq} value is obtained as a slope from the plot of I_0/I vs [Q]. In the quenching plot (inset in Fig. 4) of I_0/I *vs* [Q], the K_{sq} values were found to be 0.31 x 10^5 M^{-1}, 1.70 x 10^5 M^{-1}, 0.43 x 10^5 M^{-1} and 1.03 x 10^5 M^{-1} for complexes **1**–**4**, respectively and following the order **2** > **4** > **3** > **1** and exactly coincide with the results which obtained in the absorption studies.

Thus, based on the evidence provided by the EtBr fluorescence displacement experiments, we conclude that the complexes **1**–**4** can interact to HS-DNA through the intercalation or partial intercalation modes,[59] which is in sound agreement with results which derived from the previously discussed electronic absorption spectral measurements.

The K_{app} values (apparent binding constant) were also calculated for the complexes **1**–**4** using the equation.[61]

$$K_{EtBr}[EtBr] = K_{app}[Complex]_{50}$$

Where K_{EtBr} = 1.0 x 10^7 M^{-1} and the concentration of EtBr is 10 μM; $[complex]_{50}$ is the concentration of the complex causing 50% reduction in the emission intensity of EtBr. The K_{app} values for complexes **1**–**4** were given in Table 3. This reflects the ability of complexes to displace the EtBr from EtBr bound DNA complex through a partial intercalative interaction of the complexes **1**, **3** and **4**. Complex **2** (phen) would displaced the EtBr more efficiently than **1**, **3** and **4** by showing the higher K_{sq} and K_{app} values of **2** indicated its strong binding affinity towards HS-DNA. Moreover, the observed higher K_{app} value for the complex **4** than **1** and **3** indicates the predominant hydrophobic interaction of **4** with DNA nucleotides.

3.5.3 Electrochemical titration

Electrochemical method has been extremely useful in probing the nature and mode of DNA binding with metal complexes due to their accessible redox states.[62,63] It is well known that the redox potentials of a copper complex may shift towards more positive potential by the intercalating metallo-drugs with nucleic acid.[66]

The cyclic voltammograms of the complexes in the absence of DNA reveal a non-Nernstian with a quasi-reversible one electron Cu(II)/Cu(I) redox processes attributed from the peak potential separation of 128-280 mV (Table 4). Cyclic voltammogram of complex **3** in the absence and presence of HS-DNA in Tris-HCl buffer/MeOH solution at scan rate 100 mV/s was provided in (Fig. 5, S10-S12). All these copper complexes under investigation exhibited a negligible potential shift on titration with HS-DNA in the anodic and cathodic peaks along with the suppression of both peak currents as anticipated indicating the occurred interacalation[64] with HS-DNA through the aromatic moiety. In particular the aromatic moiety connected with sulfur atom which was not coordinated with central copper ion in the complexes **2-4** can easily penetrate into the core of DNA and the remaining portions of the complexes may stay and stick on the sugar phosphate backbone of the HS-DNA. Therefore, these observed electrochemical changes are in consistent with the non-coordinating intercalative/partial intercalative binding through the available aromatic ligand moiety between the DNA base pairs as also evidenced by the earlier deliberated spectral (UV-vis and EtBr displacement studies) results. In the absence of DNA, the E_{pc} appears at –0.005 and E_{pa} in 0.284 (ΔEp= 0.279 V, $E_{1/2}$= 0.140 V and i_{pa}/i_{pc} = 1.1) for complex **1**. E_{pc} in –0.124 and E_{pa} in 0.004 (ΔEp= 0.128 V, $E_{1/2}$= –0.060 V and i_{pa}/i_{pc} = 0.92) for complex **2**. E_{pc} in –0.205 and E_{pa} in –0.050 (ΔEp= 0.155 V, $E_{1/2}$= –0.128 V and i_{pa}/i_{pc} = 0.95) for complex **4**. The obtained results from the voltammograms illustrated that the ΔEp values are not much sensitive to the DNA addition, while there is a considerable suppression in peak current values. The formal potential, $E_{1/2}$ (voltammetric) taken as the average of E_{pc} and E_{pa}, shifted slightly towards the positive side on interaction to DNA noticed that both Cu(II) and Cu(I) forms bind to DNA at different rates. These observed electrochemical changes may due to the slow diffusion of an equilibrium mixture of the free and DNA bound complex on the electrode surface and strong interaction was occurred between them.[65,66]

Differential pulse voltammogram (DPV) experiments were also accomplished to observe the changes in the formal potentials as well as the current density during the addition of DNA to the experimental solution. The reduction process was observed at a scan rate of 100 mV s^{-1} (Fig. 6). DPV also notified the changes found in CV experiments and hence it can be concluded that the copper complex with phen ligand (**2**) was intercalate with DNA through the insertion of phen ligand between the base pairs of the DNA duplex strand.[66] Whereas, the bpy based complexes (**3** and **4**)

were interact with the DNA through the partial insertion of the aromatic rings which is connected with sulfur atom in the ligand architecture due to the lack of planarity found in bpy moiety. However, it is also notified that the complex **4** may have more possibility for hydrophobic interaction with DNA nucleotides. The suppression of current along with slight potential shift was related to the ratio of binding constants by the following equation:

$$E_b^{o'} - E_f^{o'} = 0.059\log (K_+/K_{2+})$$

where, $E_f^{o'}$ and $E_b^{o'}$ are the formal potentials of the CuL^+/CuL^{2+} couple in the free and bound forms, respectively. DPV of the complexes also showed a large decrease in current intensity with a slight shift in formal potential as a function of added DNA due to intercalative/partial intercalative interaction of complexes.

3.5.4 Circular dichroic spectral studies

To screen the potential DNA conformational changes induced by the metallo-drugs, CD spectra of HS-DNA in the absence and presence of the complexes have been recorded. The CD spectrum of B-DNA displays a positive band at 277 nm attributable to base stacking and a negative band at 246 nm that arises from the right-handed helicity of DNA.[67] If there is any modification(s) has been occurred in the base-stacking pattern or helicity of the strands may produce either a change in the band position or their intensity, or even both. It is known that simple electrostatic or groove-binding interactions of small molecules with DNA do not cause any significant alteration of the intensity of the two bands. Whereas, intercalators augment the intensity of these bands.[68] The CD spectra of HS-DNA in the presence of complexes **1**–**4** induces slight changes in both the positive and negative bands are depicted in Fig. 7. Upon addition of complexes **1**, **3** and **4** showed only minor changes on the DNA band indicated that a slight perturbation was occurred due to the partial insertion of aromatic rings as we discussed in the previous sections. Although, a significant alteration of both bands was observed by the addition of complex **2**, confirmed its intercalative mode of binding with DNA[69,70] through the sulfur containing aromatic moiety and the phen moiety.

3.6 DNA cleavage

DNA cleavage experiments were carried out using supercoiled pUC18 DNA using agarose gel electrophoresis. In the control experiment using ascorbic acid in the absence of complexes, no characteristic cleavage of DNA was observed. Whereas, the cleaved fragments of DNA were observed for the complexes **1**–**4** in the presence of ascorbic acid showed, visualized under UV lamp and photographed. Complexes **1**–**4** can able to cleave SC (Form I) DNA into nicked circular form

(NC) (Form II) [Fig. 8] in the presence of ascorbic acid, and the observed cleavage efficiency follows the order of **2** > **4** > **3** > **1** depending upon the co-ligand. The effect of the DNA cleavage by complex **2** was studied at lower concentration (30 μM) (lane 5, Fig. 8b), since it showed better DNA interaction among other complexes, as anticipated the increasing concentration of **2** induced the DNA cleavage more efficiently, it was monitored by the appearance of Form II while the disappearance of Form I. These observations clearly noticed that the formation of Cu(I) species in the complex **2** even at lower concentration compared to other complexes root to enhance intense nuclease activity. Moreover, it is also noticed that the hydrophobicity of the complex **4** may induces efficient fragmentation of the DNA next to complex **2** and better than complexes **1** and **3**.

The efficient nuclease activity of **2** is speciously due to the enhanced stabilization its Cu(I) species formed by ascorbic acid, moreover the hydrophobic nature of phen ligand also plays an important role. As previously reported, Cu(I) species can have more DNA binding affinity than Cu(II) species,[71] so, the interactions through π-stacking is also an important factor for efficient DNA cleavage. This study reveals that **2** cleaves DNA more efficiently than the other complexes, because of the strong interaction of the extended aromatic rings of the phen moiety.[72]

3.7 Molecular docking studies with DNA

All the copper(II) complexes were subjected to molecular docking with DNA using the AutoDock Tools to confirm the results observed from spectral and electrochemical analysis. Complexes **1**–**4** were analysed for their docking conformation in terms of energy, hydrogen bonding, and hydrophobic interactions towards DNA. The observed results reveal that all the docked complexes can fit into the DNA more conveniently by contact with DNA functional groups, however they did not disrupt the DNA double helical, which resulted in the binding energy values of –4.62, –4.83, –4.32 and –4.72 kcal mol^{-1} respectively for compelxes **1**–**4** (Table 5). Complex **2** showed a higher binding energy of –4.83 kcal mol^{-1}. The decreasing order of binding energy is closely comparable with results obtained from the formerly discussed spectral and electrochemical techniques. It is also noticed that the complexes **1** and **4** were bound in the region of GC-TA, whereas, complexes **2** and **3** were bound in the region of GC-GC residues.[38] Fig. 9 illustrated the docked models. Docking protocol was validated with the removal of ClO_4 from complex **4** and again docked back (Fig. S13 and Table S1).

3.8 Protein binding studies

3.8.1 Fluorescence quenching measurements

Currently, the interactions between the maximum abundant blood plasma protein, serum albumin (BSA/HSA), and metallo-drugs have attracted immense interest because of its structural homology with human serum albumin. Moreover, the interaction of these metallo-drugs to the proteins may lead to either a loss or an enhanced the biological functions of the original drug. It exhibits essential fluorescence due of the presence of different aromatic amino acids such as phenylalanine, tyrosine, and tryptophan abundantly. The fluorescence of BSA will be completely reduced during the ionization of tyrosine, whereas phenylalanine has a very low quantum yield. This clearly indicated that the intrinsic fluorescence behaviour of BSA is mainly due to the presence of tryptophan and tyrosine. The fluorescence intensity of BSA will appear mostly due to the most environmentally exposed tryptophan residues during its excitation at 295 nm.[73] Therefore, the fluorescent behaviour of BSA can provide significant information about the structure, dynamics, and protein folding. A solution of BSA (1 μM) was titrated with various concentrations of the complexes, (0–20 μM) in the range of 290–450 nm (λ_{exc} 280 nm). The effect of increasing concentration of complexes on the fluorescence emission of BSA was illustrated in the Fig. 10. Titration of all these complexes with the solution of BSA resulted in a significant decrease of its intrinsic fluorescence intensity at 348 nm along with the slight blue shift (1-3 nm). This obtained blue shift primarily arises due to the presence of the active site of protein in a hydrophobic environment. These results suggested that a strong interaction may occur between all the complexes and BSA. The fluorescence quenching is described by Stern-Volmer relation:

$$I_0/I = K_{sv}[Q] + 1$$

Where I_0 is the emission intensity of the absence of quencher, I is the emission intensity of the presence of quencher, K_{sv} is the Stern-Volmer quenching constant, [Q] is the quencher concentration. K_{sv} is the slope obtained from the plot I_0/I *versus* [Q] (Shown if Fig. 11).

Further, the equilibrium binding constant was evaluated using the Scatchard equation: [74,75]

$$\log[(F_0 - F)/F] = \log K_b + n \log [Q]$$

Where F_0 and F are the fluorescence intensities in the absence and presence of quencher, [Q] is the concentration of quencher, K_b and n are the binding constant and the number on binding sites, respectively. The plot of $\log[(F_0 - F)/F]$ *versus* $\log [Q]$ can be used to determine the values of both K_b as well as n and the calculated values for complexes **1**–**4** shown in Fig. 12 and the observed data have been listed in Table 6. The estimated value of n (~ 1) strongly supported the existence of a single binding site in BSA. The obtained results from the fluorescence spectra clearly showed that

the complex **3** has higher binding constant value compared to the other complexes and the observed order of binding efficiency is **3** > **2** > **1** > **4**.

3.8.2 UV-visible absorption studies

UV-vis absorption spectroscopy is the tool to explore the structural change and the type of quenching BSA by the drug molecules. In common, quenching may occurs either by dynamic or static mode. Static quenching denotes the formation of a fluorophore (BSA)-quencher complex in the ground state, whereas dynamic quenching is a process in which the fluorophore and the quencher come into contact during the transient existence of the excited state.[76,77] The UV absorption spectrum of pure BSA and BSA-complex (**1**–**4**) are shown in Fig. 13. It clearly displays that, the absorption intensity of BSA appeared at 279 nm was enormously enhanced due to the addition of metal complexes along with little blue shift (~ 2 nm) for all these copper(II) complexes. It suggested that a static interaction was occurred between BSA and the copper(II) complexes in the ground state as previous report.[57,58] But, dynamic quenching affects only the excited state while it has no function on the absorption spectrum.

3.9 Cytotoxicity

The *in vitro* cytotoxic activity of the complexes **1**–**4** with A549 (lung cancer cells) and Huh7 (liver cancer cells) cells has been studied using MTT assay. Inhibitory concentrations of complexes were found based on dosage dependent cell viability. Cytotoxicity of complexes **1** and **3** were exhibited high cytotoxicity against A549 and Huh7 cell lines after the incubation for 24 h [IC_{50} = 26.45 μM (A549) and 38.27 μM (Huh7)][78] and the results were given in Fig. 14 and 15. Whereas complexes **2** and **4** were least cytotoxicity against A549 and Huh7 cell lines comparably to the complexes **1** and **3.** However complexes **1-4** showed enhanced cytotoxicity than the ligand. Among the complexes **1-4**, complex **1** has been claimed the efficient anticancer property. Inhibitory concentration values [IC_{50}] of all the complexes **1-4** along with the probe are listed in Table 7.

4. Conclusion

A series of copper(II) complexes (**1**–**4**) with a simple and mixed ligands have been synthesized and characterized by analytical, spectral, electrochemical and single crystal X-ray diffraction techniques with a view to evaluate their biological applications. The single crystal X-ray crystallography of complex **4** reveals the presence of a square planar geometry around the copper centre with slight distortion. The K_b values obtained from absorption studies stated that the DNA

binding ability was in the order of **2** > **4** > **3** > **1**. These observed results demonstrated that their effective interactions with DNA base pairs in the minor groove through the strong partial intercalation mode due to the presence of aromatic rings in the ligand architecture and phen / bpy co-ligands. Whereas, the dmbpy complex may have a significant hydrophobic interaction with DNA through the methyl groups on bpy ring, which is relevant to the obtained higher binding constant than bpy complex.

All the complexes cleave the supercoiled pUC18-DNA into nicked circular form in the presence of ascorbic acid as a reducing agent and the phen complex exhibit better cleavage efficiencies than those of the other complexes. In addition, the UV−visible and fluorescence spectroscopic results revealed that these complexes interact with serum protein (BSA) through static mode. The molecular docking studies also confirmed the partial insertion of these complexes with DNA backbone. Moreover, it is well known that the metal complexes containing sulfur atom connected to the metal centre might have shown better biological applications, whereas the copper complexes under investigated in this manuscript also have shown a very significant biological properties though the S-donor atom did not coordinated with the central copper atom. These observed results may due to the planarity and hydrophobicity of the diimine co-ligands. All these complexes have a significant cytotoxicity against A549 and Huh7 cancer cell lines.

Acknowledgements

The authors Dr J. A and S. K gratefully acknowledge Department of Science and Technology (DST), New Delhi [Grant No: SB/FT/CS-175/2011] and the UGC, New Delhi [F.No. 42-247/2013 (SR) dated 12-03-2013] for financial support.

References

1 Z. Guo and P. J. Sadler, *Angew. Chem. Int. Ed.* 1999, **38**, 1512–1531.

2 B. Rosenberg, L. Vam Camp, J. E. Trosko and V. H. Mansour, *Nature,* 1969, **222**, 385–386.

3 Z. Wu, Q. Liu, X. Liang, X. Yang, N. Wang, X. Wang, H. Sun, Y. Lu and Z. Guo, *J. Biol. Inorg. Chem.,* 2009, **14**, 1313–1323.

4 D. S. Raja, N. S. P. Bhuvanesh and K. Natarajan, *Dalton Trans*., 2012, **41**, 4365–4377.

5 M. Jin Li, T. Yu Lan, X. Hui Cao, H. Hao Yang, Y. Shi, C. Yi and G. Nan Chen, *Dalton Trans*., 2014, **43**, 2789–2798.

6 E. Wong and C. M. Giandomenico, *Chem. Rev.,* 1999, **99**, 2451–2466.

7 A. M. Angeles Boza, P. M. Bradley, P. K. L. Fu, S. E. Wicke, J. Bacsa, K. M. Dunbar and C. Turro, *Inorg. Chem*., 2004, **43**, 8510–8519.

8 P. J. Bednarski, F. S. Mackay and P. J. Sadler, *Med. Chem*., 2007, **7**, 75-93.

9 Y. B. Zeng, N. Yang, W. S. Liu and N. Tang, *J. Inorg. Biochem*., 2003, **97**, 258–264.

10 V. S. Li, D. Choi, Z. Wang, L. S. Jimenez, M. S. Tang and H. Kohn, *J. Am. Chem. Soc.*, 1996, **18**, 2326–2331.

11 G. Zuber, J. C. Quada and S. M. Hecht, *J. Am. Chem. Soc.*, 1998, **120**, 9368–9369.

12 S. M. Hecht, *J. Nat. Prod*., 2000, **63**, 158–168.

13 J. C. G. Ramos, R. G. Murillo, F. C. Guzmán and L. R. Azuara, *J. Mex. Chem. Soc*., 2013, **57**, 245-259.

14 P. Kalaivani, R. Prabhakaran, E. Vaishnavi, T. Rueffer, H. Lang, P. Poornima, R. Renganathan, V. Vijaya Padma and K. Natarajan, *Inorg. Chem. Front*., 2014, **1**, 311–324.

15 M. Alagesan, N. S. P. Bhuvanesh and N. Dharmaraj, *Dalton Trans*., 2013, **42**, 7210–7223.

16 C. Santini, M. Pellei, V. Gandin, M. Porchia, F. Tisato and C. Marzano, *Chem. Rev*., 2014, **114**, 815-862.

17 L. R. Azuara, G. ME Bravo, *Curr Med Chem*., 2010, **1**7, 3606-3615.

18 B. P. Esposito and R. Najjar, *Coord. Chem. Rev.*, 2002, **232**, 137–149.

19 J. Seetharamappa and B. P. Kamat, *Chem. Pharm. Bull*., 2004, **52**, 1053–1057.

20 E. Sundaravadivel, S. Vedavalli, M. Kandaswamy, B. Varghese and P. Madankumar, *RSC.Adv*., 2014, **4**, 40763-40775.

21 T. M. Sielecki, J. F. Boylan, P. A. Benfield and G. L. Trainor, *J. Med. Chem*., 1999, **43**, 1–18.

22 Z. Zang, L. Jin, X. Qian, M. Wei, Y. Wang, J. Wang, Y. Yang, Q. Xu, Y. Xu and F. Liu, *ChemBioChem.*, 2007, **8**, 113–121.

23 S. Sarkar, P. K. Dhara, M. Nethaji and P. Chattopadhyay, *J. Coord. Chem.*, 2009, **62**, 817–824.

24 (a) H. Goldie and M. D. Felix, *Cancer Res*. 1951, **11**, 73–80; (b) X. Wang and Z. Guo, *Med. Chem*., 2007, **7**, 19–34; (c) C. Jacob, G.I. Giles, N.M. Giles and H. Sies, *Angew. Chem. Int. Ed.,* 2003, **42**, 4742–4758.

25 J. D. Ranford, P. J. Sadler and D. A. Tocher, *Dalton Trans*., 1993, **22**, 3393–3399.

26 S. Ramakrishnan, V. Rajendiran, M. Palaniandavar, V. S. Periasamay, M. A. Akbarsha, B. S. Srinag and H. Krishnamurthy, *Inorg. Chem.,* 2009, **48**, 1309–1322.

27 S. Ramakrishnan, D. Shakthipriya, E. Suresh, V.S. Periasamy, M.A. Akbarsha and M. Palaniandavar, *Inorg. Chem*., 2011, **50**, 6458–6471.

28 R. Loganathan, S. Ramakrishnan, E. Suresh, A. Riyasdeen, M. A. Akbarsha and M. Palaniandavar, *Inorg. Chem*., 2012, **51**, 5512–5532.

29 M. Chikira, Y. Tomizava, D. Fukita, T. Sugizaki, N. Sugawara, T.Yamazaki, A. Sasano, S. Shindo, M. Palaniandavar and W. Anthroline, E. *J. Inorg. Biochem.,* 2002, **89**, 163–173.

30 B. Selvakumar, V. Rajendiran, P. U. Maheswari, H. S. Evans and M. Palaniandavar, *J. Inorg. Biochem.,* 2006, **100**, 316–330.

31 A. C. T. North, D. C. Phillips and F. S. Mathews, *Acta Cryst. Sect. A,* 1968, **24**, 348–351.

32 G. M. Sheldrick, SHELXL97 and SHELXS97, 1997, University of Gottingen, Germany.

33 L. J. Farrugia, *J. Appl. Cryst*. B 1997, **30**, 565–566.

34 A. Meenongwa, R. F. Brissos, C. Soikum, P. Chaveerach, P. Gamez, Y. Trongpanich and U. Chaveerach, *New. J. Chem*., 2015, **39**, 664–675.

35 M. F. Shubsda, J. Goodisman and J. C. Dabrowiak, *J. Biochem. Biophys. Methods.*, 1997, **34**, 73–79.

36 D. Shao, M. Shi, Q. Zhao, J. Wen, Z. Geng, and Z. Wang, Z. *Anorg. Allg. Chem.,* 2015, **641**, 454–459.

37 V. Thamilarasan, A. Jayamani and N. Sengottuvelan, *Eur. J. Med. Chem*., 2015, **89**, 266–278.

38 M. J. Frisch, G.W. Trucks, H. B. Schlegel, G. E. Scuseria, M. A. Robb, J. R. Cheeseman, G. Scalmani, V. Barone, B. Mennucci, G. A. Petersson, H. Nakatsuji, M. Caricato, X. Li, H. P. Hratchian, A. F. Izmaylov, J. Bloino, G. Zheng, J. L. Sonnenberg, M. Hada, M. Ehara, K. Toyota, R. Fukuda, J. Hasegawa, M. Ishida, T. Nakajima, Y. Honda, O. Kitao, H. Nakai, T. Vreven, J. A. Montgomery Jr., J. E. Peralta, F. Ogliaro, M. Bearpark, J. J. Heyd, E. Brothers, K. N. Kudin, V. N. Staroverov, R. Kobayashi, J. Normand, K. Raghavachari, A. Rendell, J. C. Burant, S. S. Iyengar, J. Tomasi, M. Cossi, N. Rega, J. M. Millam, M. Klene, J. E. Knox, J. B. Cross, V. Bakken, C. Adamo, J. Jaramillo, R. Gomperts, R. E. Stratmann, O. Yazyev, A. J. Austin, R. Cammi, C. Pomelli, J. W. Ochterski, R. L. Martin, K. Morokuma, V. G. Zakrzewski, G. A. Voth, P. Salvador, J. J. Dannenberg, S. Dapprich, A. D. Daniels, Ö. Farkas, J. B. Foresman, J. V. Ortiz, J. Cioslowski and D. J. Fox. Gaussian Inc, Wallingford, CT 2009.

39 K. P. S. Adinarayana and R. K. Devi, *Bioinformation*., 2011, **6**, 74-77.

40 J. Haribabu, K. Jeyalakshmi, Y. Arun, Nattamai. S. P. Bhuvanesh, P. T. Perumal and R. Karvembu, *RSC Adv*., 2015, **5**, 46031-46049.

41 T. Mossman, *J. Immunol. Methods*, 1983, **65**, 55–63.

42 M. Kalita, T. Bhattacharjee, P. Gogoi, P. Barman, R. D. Kalita, B. Sarma and S. Karmakar, *Polyhedron*., 2013, **60**, 47-53.

43 T. Rosu, E. Pahontu, C. Maxim, R. Georgescu, N. Stanica and A. Gulea, *Polyhedron.*, 2011, **30**, 154–162.

44 P. M. Krishna and K. H. Reddy, *Inorg. Chim. Acta*, 2009, **362**, 4185–4190.

45 R. Saswati, C. S. Dinda, E. Schmiesing, Y. P. Sinn, M. Patil, H. Nethaji, E. Stoeckli and R. Acharyya, *Polyhedron.*, 2013, **50,** 354–363.

46 D. Lahiri, R. Majumdar, D. Halleck, T. K. Goswami Rajan R. Dighe and A. R. Chakravarty, *J. Inorg. Biochem*., 2011, **105**, 1086–1094.

47 R. R. Pulimamidi, R. Nomula, R. Pallepogu and H. Shaik, *Eur. J. Med. Chem.*, 2014, **79**, 117–127.

48 T. Gupta, S. Dhar, M. Nethaji and A. Chakravarty, *Dalton Trans*., 2004, 1896–1900.

49 (a) Q. L. Zhang, J. G. Liu, H. Chao, G. Q. Xue and L. N. Ji, *J. Inorg. Biochem*., 2001, **83**, 49–55; (b) Z. C. Liu, B. D. Wang, B. Li, Q. Wang, Z. Y. Yang, T. R. Li and Y. Li, *Eur. J. Med. Chem*., 2010, **45**, 5353–5361.

50 P. Krishnamoorthy, P. Sathyadevi, R. R. Butorac, A. H. Cowley, Nattamai S. P. Bhuvanesh and N. Dharmaraj, *Dalton Trans*., 2012, **41**, 4423-4436.

51 J. G. Liu, Q. L. Zhang and L. N. Ji, *Transition Met. Chem.,* 2001, **26**, 733–738.

52 Chan, H. L.; Liu, H. Q.; Tzeng, B. C.; You, Y. S.; Peng, S. M.; Yang, M.; Che, C. M. Inorg. Chem. 2002, **41**, 3161-3171.

53 (a) V. Rajendiran, R. Karthik, M. Palaniandavar, H. S. Evans, V. S. Periasamy, M. A. Akbarsha, B. S. Srinag and H. Krishnamurthy, *Inorg. Chem.,* 2007, **46**, 8208–8221; (b) V. Rajendiran, M. Palaniandavar, P. Swaminathan and L. Uma, *Inorg. Chem*., 2007, **46**, 10446–10448.

54 R. Loganathan, S. Ramakrishnan, E. Suresh, M. Palaniandavar, A. Riyasdeen and M. A. Akbarsha, *Dalton Trans.,* 2014, **43**, 6177–6194.

55 M. J. Waring, *J. Mol. Biol*. 1965, **13**, 269–282.

56 I. Changzheng, W. Jigui, W. Liufang, R. Min, J. Naiyang and G. Jie, *J. Inorg. Biochem*., 1999, **73**, 195–202.

57 J. R. Lakowicz and G. Weber, *Biochemistry.,* 1973, **12**, 4161–4170.

58 K. Jeyalakshmi, Y. Arun, N. S. P. Bhuvanesh, P. T. Perumal, A. Sreekantha and R. Karvembu, *Inorg. Chem. Front*., 2015, **2**, 780-798.

59 M. Ganeshpandian , S. Ramakrishnan, M. Palaniandavar, E. Suresh, A. Riyasdeen and M. A. Akbarsha, *J. Inorg. Biochem*., 2014, **140**, 202-212.

60 A. Barve, A. Kumbhar, M. Bhat, B. Joshi, R. Butcher, U. Sonawane and R. Joshi, *Inorg. Chem*., 2009, **48**, 9120-9132.

61 R. K. Gupta, G. Sharma, R. Pandey, A. Kumar, B. Koch, P. Z. Li, Q. Xu, and D. S. Pandey, *Inorg. Chem*., 2013, **52**, 13984-13996.

62 S. Mahadevan and M. Palaniandavar, *Inorg. Chem*., 1998, **37**, 693–700.

63 M. Sirajuddin, S. Ali, and A. Badshah, *J. Photochem. Photobio., B,* 2013, **124**, 1–19.

64 Y. Song, P. Yang, M. Yang, J. Kang, S. Qin, B. Lu and L. Wang, *Transition Met. Chem*., 2003, **28**, 712–716.

65 J. Lakshmipraba, S. Arunachalam, A. Riyasdeen, R. Dhivya and M. A. Akbarsha, *J. Photochem. Photobio*., B, 2015, **142**, 59-67.

66 (a) J. Annaraj, S. Srinivasan, K. M. Ponvel and PR. Athappan, *J. Inorg. Biochem*., 2005, **99**, 669–676.

67 L. Li, Q. Guo, J. Dong, T. Xu and J. Li, *J. Photochem. Photobiol., B*, 2013, **125**, 56-62.

68 (a) S. Kathiresan, T. Anand, S. Mugesh and J. Annaraj, *J. Photochem. Photobiol*, *B,* 2015, **148**, 290–301; (b) H. Pezzano and F. Podo, *Chem. Rev.,* 1980, **80**, 365–401; (c) B. Saha, Md. M. Islam, S. Paul, S. Samanta, S. Ray, C. R. Santra, S. R. Choudhury, B. Dey, A. Das, S. Ghosh, S. Mukhopadhyay, G. S. Kumar and P. Karmakar, *J. Phys. Chem. B,* 2010, **114**, 5851–5861.

69 S. Schäfer, I. Ott, R. Gust and W.S. Sheldrick, *Eur. J. Inorg. Chem.,* 2007, **2007**, 3034–3046.

70 S. Ramakrishnan and M. Palaniandavar, *Dalton Trans*., 2008, 3866-3878.

71 S. Mahadevan and M. Palaniandavar, *Inorg. Chem*., 1998, **37**, 3927–3934.

72 S. Ramakrishnan, D. Shakthipriya, E. Suresh, V. S. Periasamy, M. A. Akbarsha and M. Palaniandavar, *Inorg. Chem*., 2011, **50**, 6458–6471.

73 C. V. Dang, R. F. Ebert and W. R. Bell, *J. Biol. Chem*., 1985, **260**, 9713–9719.

74 E. Sundaravadivel, S. Vedavalli, M. Kandaswamy, B. Varghese and P. Madankumar, *RSC Adv*., 2014, **4**, 40763-40775.

75 J. Lu, Q. Sun, J. L. Li, L. Jiang, W. Gu, X. Liu, J. L. Tian and S. P. Yan, *J. Inorg. Chem*., 2014, **137**, 46-56.

76 (a) E. Ramachandran, D. S. Raja, N. S. P. Bhuvanesh and K. Natarajan, *Dalton Trans*., 2012, **41**, 13308–13323; (b) D. S. Raja, N. S. P. Bhuvanesh and K. Natarajan, *Dalton Trans.,* 2012, **41**, 4365–4377.

77 D. S. Raja, G. Paramaguru, N. S. P. Bhuvanesh, J. H. Reibenspies, R. Renganathan and K. Natarajan, *Dalton Trans.,* 2011, **40**, 4548–4559.

78 T. K. Goswami, B. V. Chakravarthi, M. Roy, A. A. Karande and A. R. Chakravarty, *Inorg. Chem*., 2011, **50**, 8452–8464.

Figures

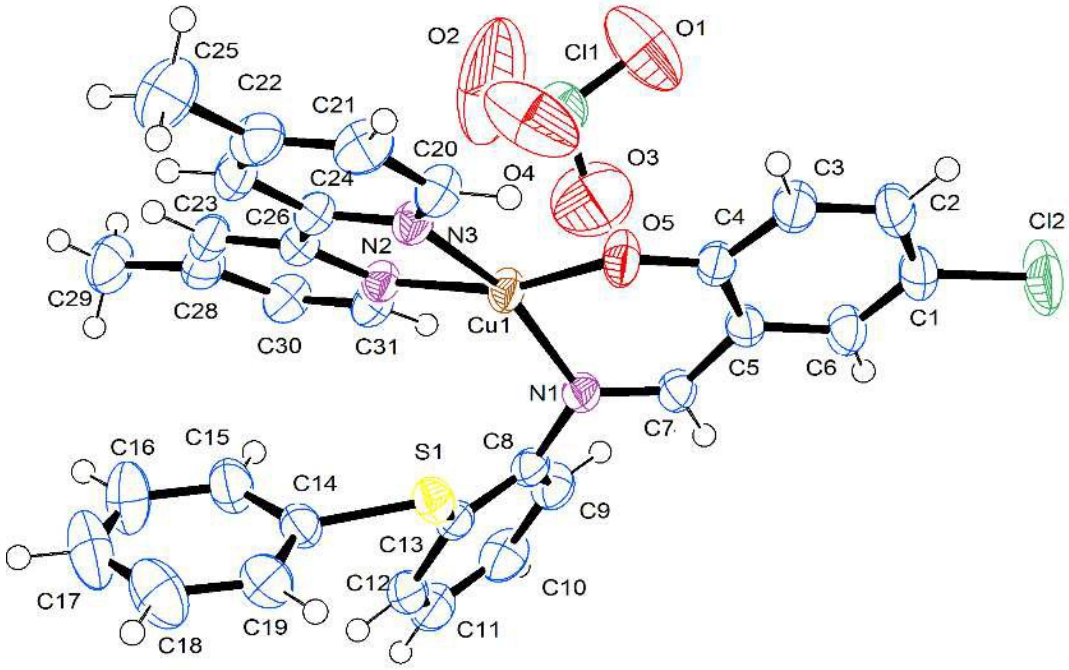

Fig. 1 ORTEP diagram of [Cu(L)(dmbpy)]ClO_4 **(4)** with the atom labeling scheme.

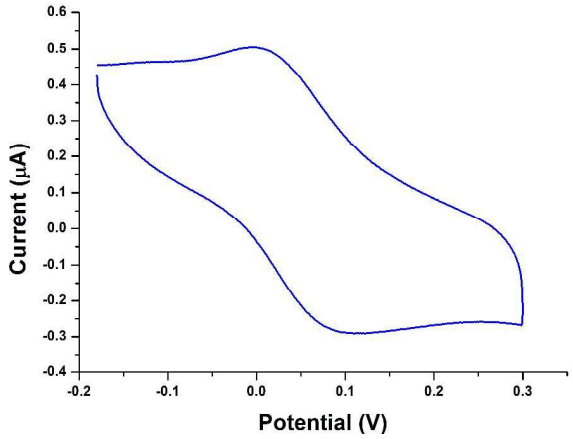

Fig. 2 Cyclic voltammogram of complex **2** in CH_3CN (0.1 M TBAP) on a GC working electrode with scan rate of 100 mV s^{-1}.

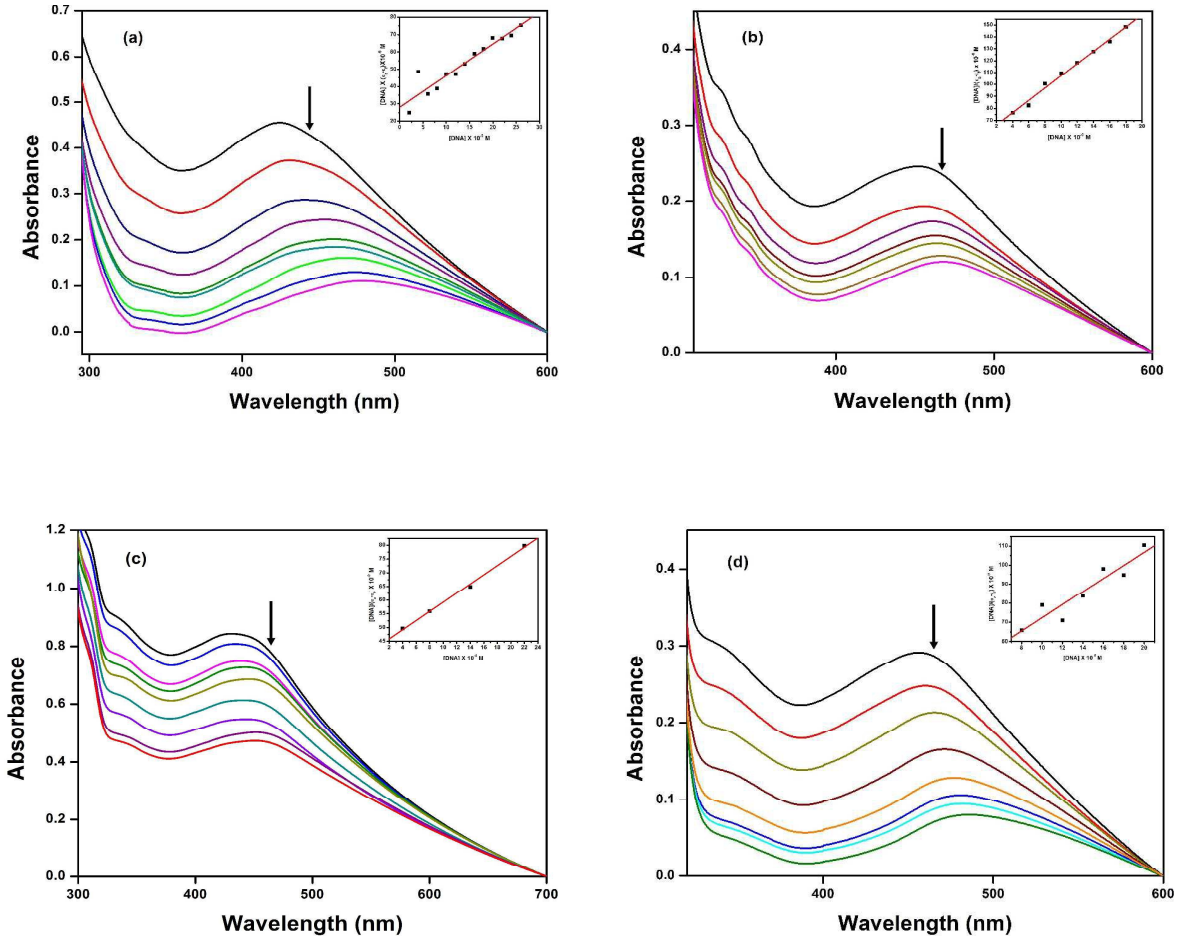

Fig. **3** Absorption spectra of complexes (a) **1**, (b) **2**, (c) **3** and (d) **4** in Tris-HCl buffer with increasing concentrations of HS-DNA. The arrow indicates that the decreasing absorption intensity upon increasing concentrations of DNA, the inset shows the binding isotherms with HS-DNA.

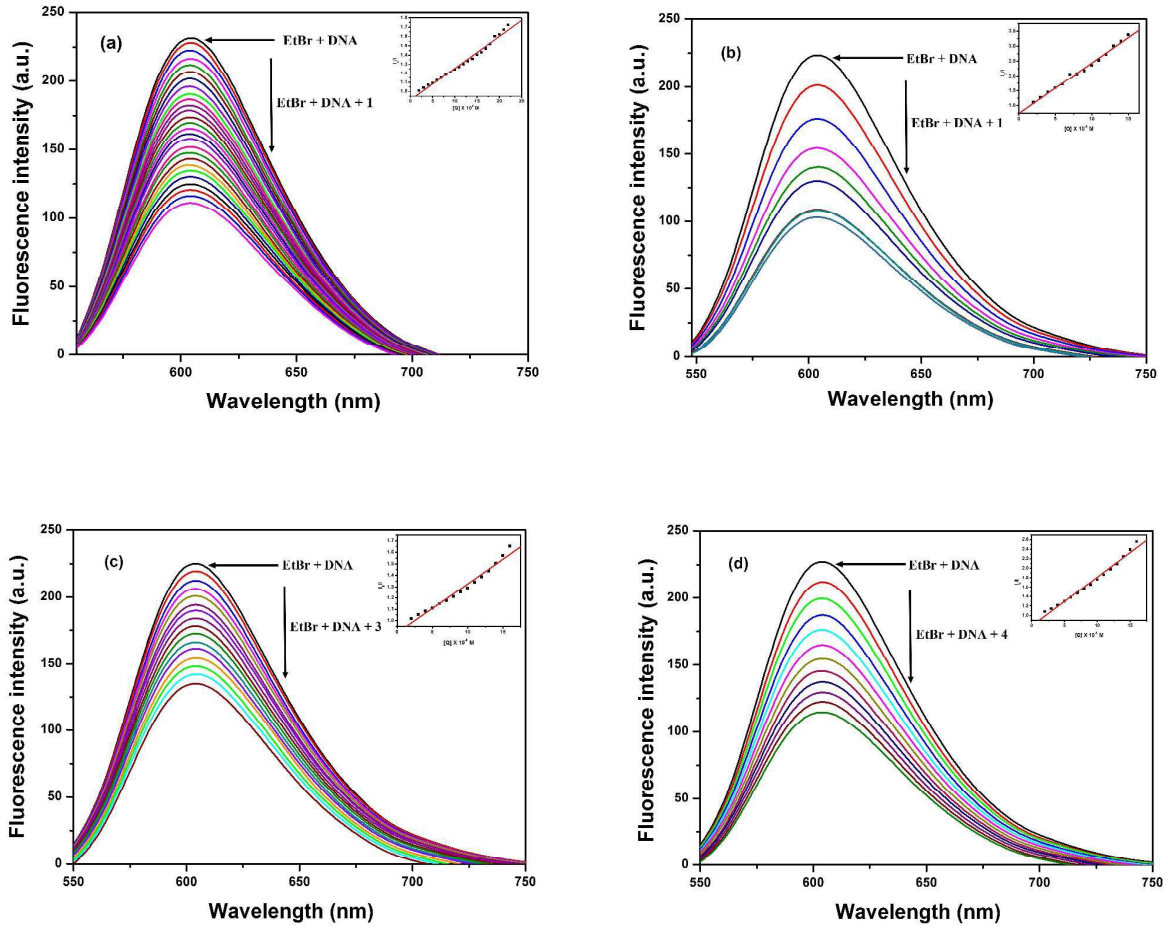

Fig. 4. Fluorescence quenching curves of EtBr bound to DNA in the presence of (a) **1**, (b) **2**, (c) **3** and (d) **4**. [DNA] = 5 μM, [EtBr] = 10 μM and [complex] = 0-150 μM. Inset shows the Stern-Volmer quenching curve.

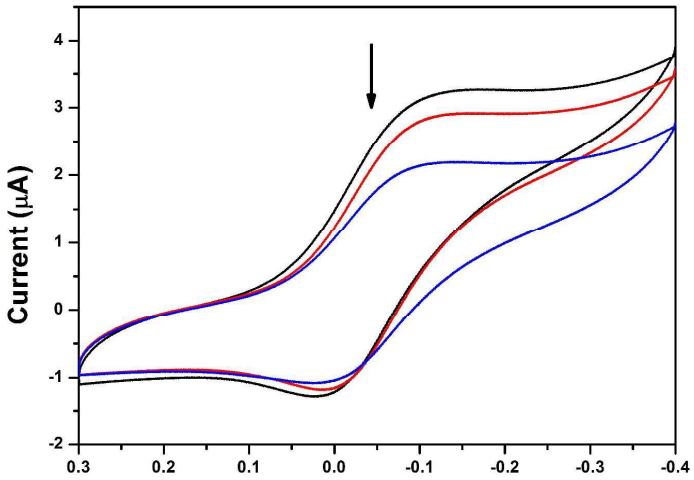

Fig. 5 Cyclic voltammograms of complex **3** in the absence and presence of HS-DNA at scan rate of 100 mV s^{-1} (Tris-HCl buffer, pH 7.1).

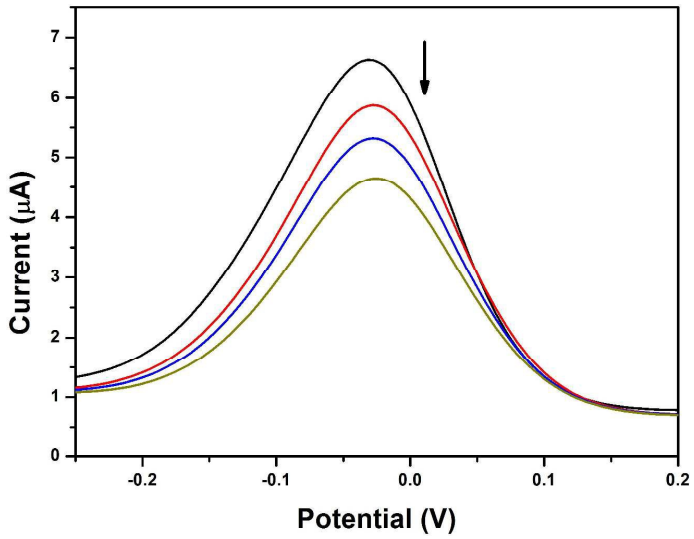

Fig. 6 Differential pulse voltammogram of **3** in the absence and presence of HS-DNA at scan rate of 100 mV s^{-1} (Tris-HCl buffer, pH 7.1). The arrow indicates the voltammetric current changes upon increasing DNA concentration.

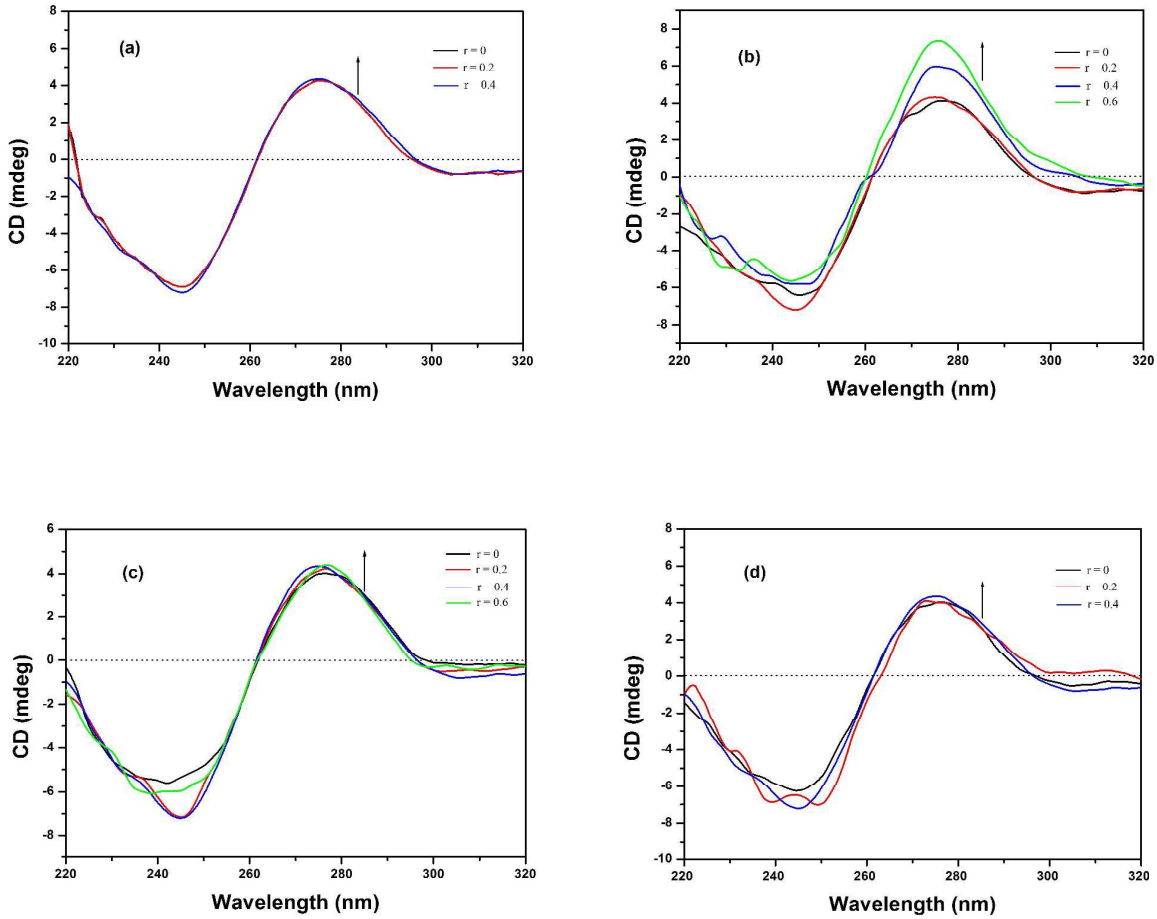

Fig. 7 CD spectra of HS-DNA (100 μM) in the absence and presence of (a) **1**, (b) **2**, (c) **3** and (d) **4** in Tris-HCl buffer at room temperature.

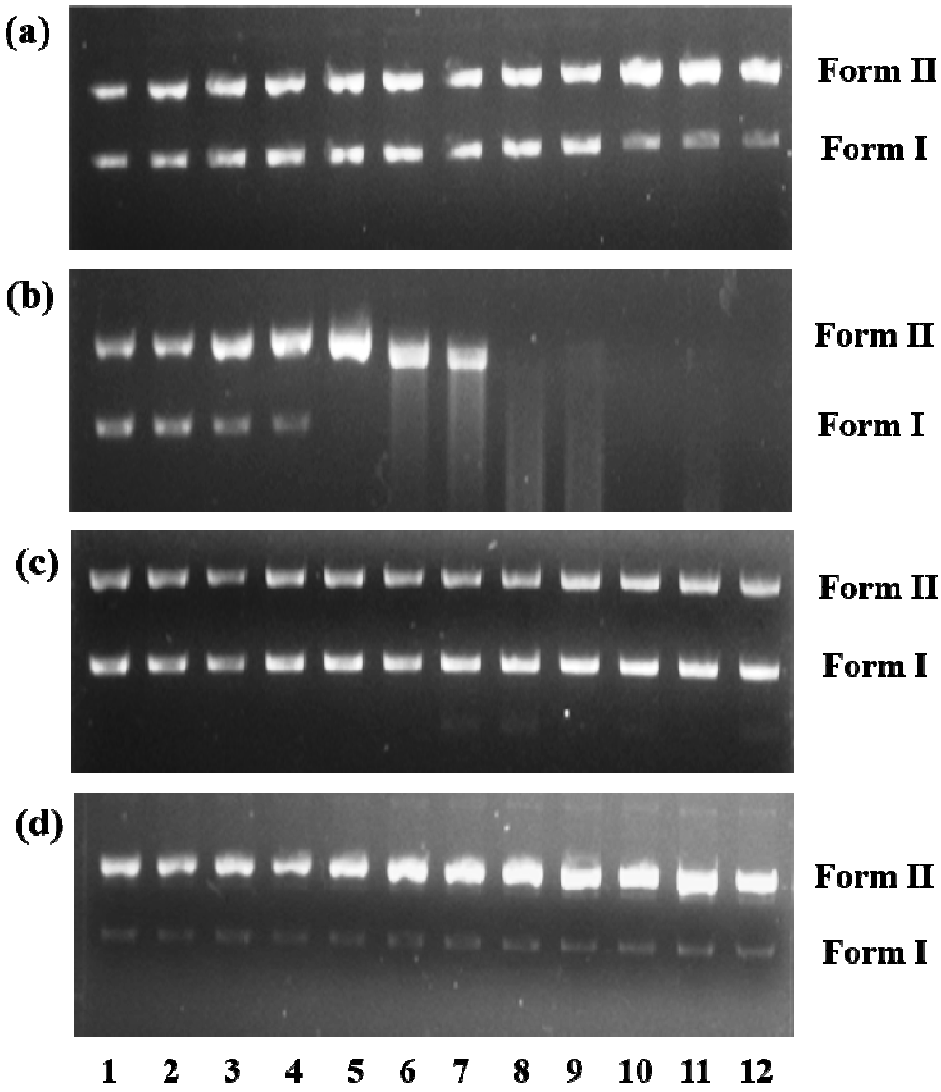

Fig. 8 Cleavage of supercoiled pUC18 DNA incubated for 1 h at 37 ^{o}C in Tris-buffer (5 mM Tris-HCl/ 50 mM NaCl, pH = 7.12) with increasing concentration of **1** (a), **2** (b), **3** (c) and **4** (d) in the presence of a reducing agent, *i.e.* ascorbic acid (H_2A; 100 μM). Lane 1: DNA control; lane 2: DNA + H_2A; lane: 3–12: DNA + H_2A + [complex] (10, 20, 30, 40, 50, 60, 70, 80, 90 and 100 μM, respectively).

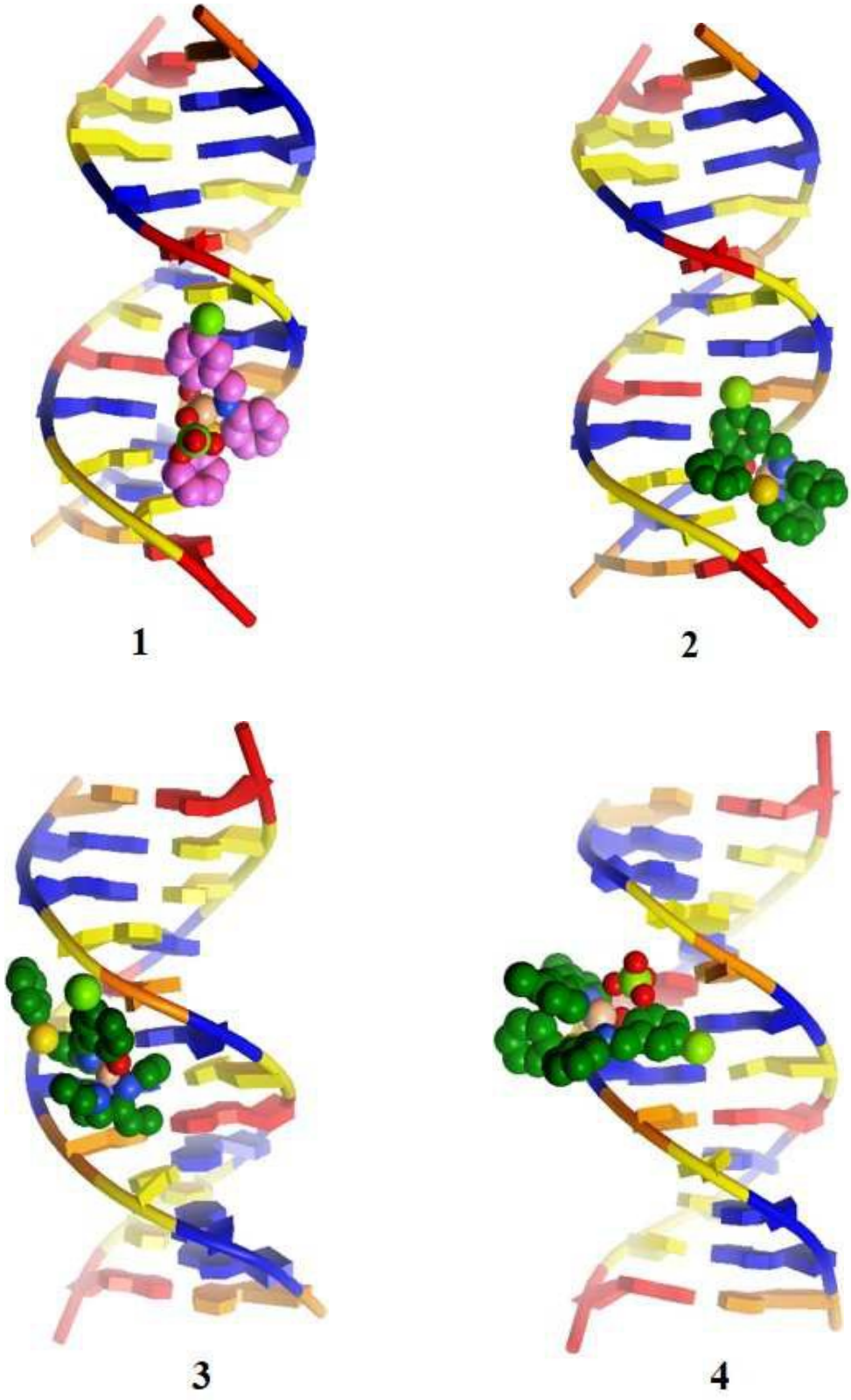

Fig. 9 Molecular docked model of complex **1**–**4** with DNA (PDB ID: 423D).

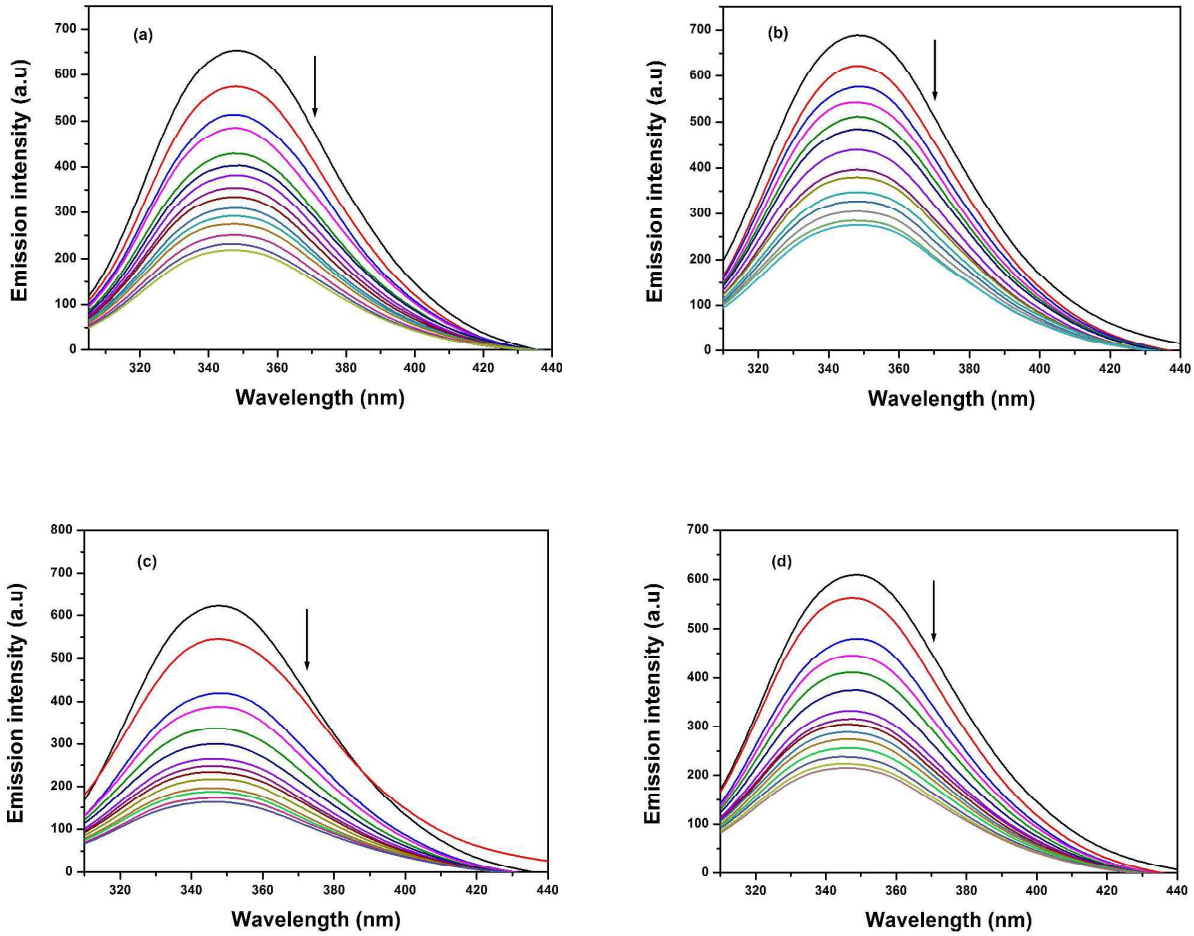

Fig. 10 Fluorescence quenching curves of BSA (black solid line) in the absence and presence (other lines) of complexes (a) **1**, (b) **2**, (c) **3** and (d) **4**. [BSA] = 1 μM and [complexes] = 0–20 μM.

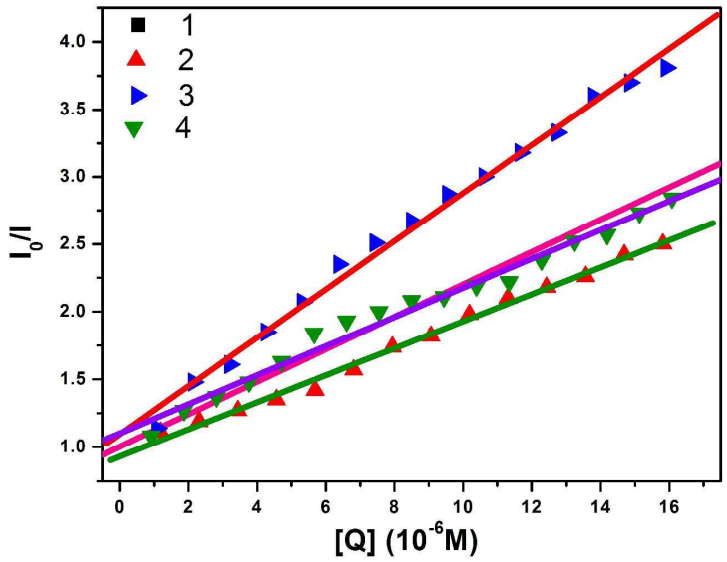

Fig. 11 Stern-Volmer plots of the fluorescence titrations of the complexes (**1**–**4**) with BSA.

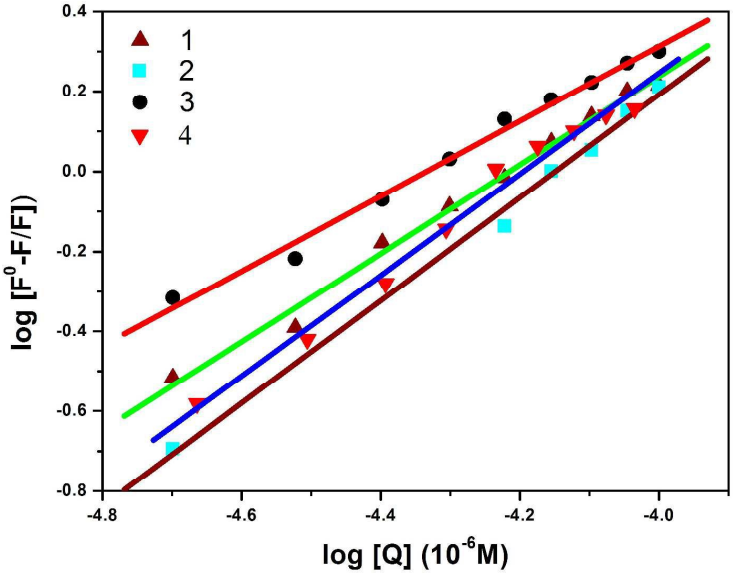

Fig. 12 Scatchard plots of the fluorescence titrations of the complexes (**1**–**4**) with BSA.

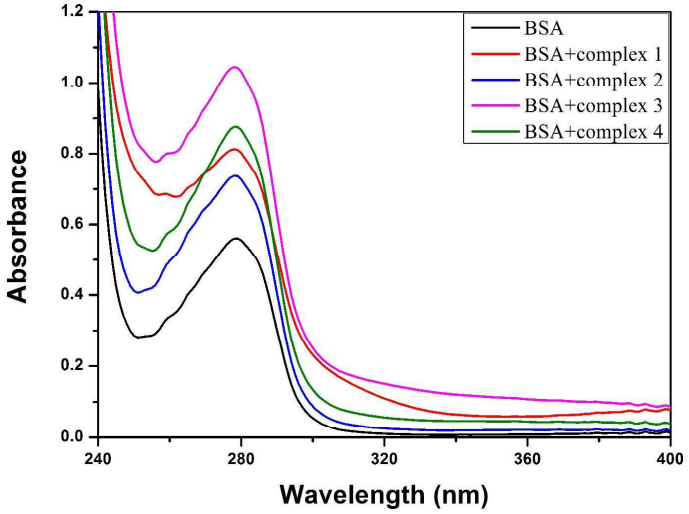

Figure. 13 The absorption spectra of BSA (Tris-HCl buffer, 10 μM, pH =7.1) and BSA with **1**–**4** (5 μM).

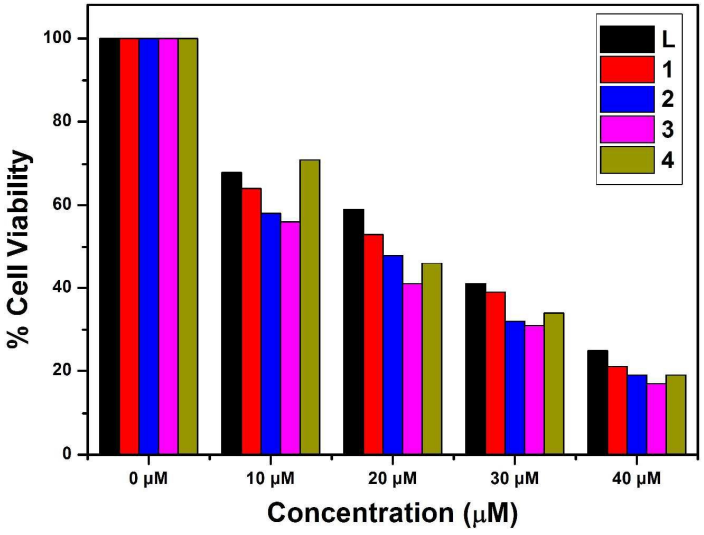

Fig. 14 Cytotoxicity of L and complexes **1**–**4** after 24 h incubation on A549 cell lines.

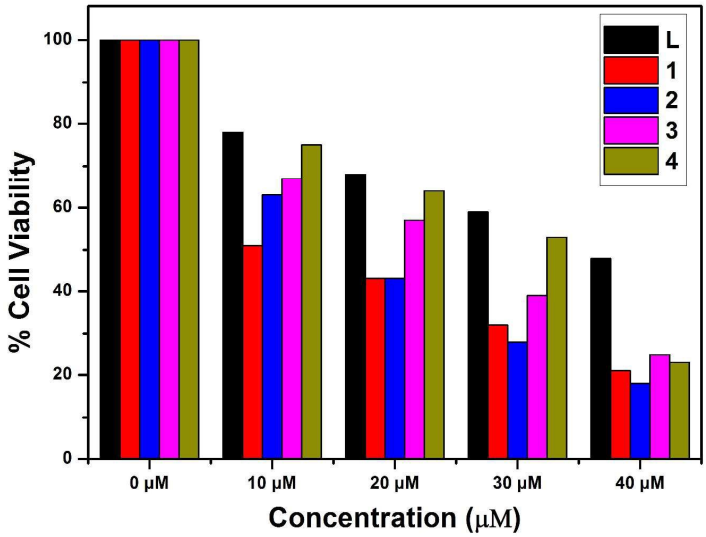

Fig. 15 Cytotoxicity of L and complexes **1**–**4** after 24 h incubation on Huh7 cell lines.

Table 1 Crystallographic data and structure refinement for complex **4**

Empirical formula	$C_{31}H_{25}Cl_2CuN_3O_5S$
Formula weight	686.04
Temperature (K)	293(2)
Wavelength (Å)	0.71073
Crystal system	Triclinic
Space group	$P\bar{1}$
Unit cell dimensions	
a (Å)	10.025
b (Å)	13.171
c (Å)	13.409
α (°)	66.74
β (°)	82.90
γ (°)	68.04
Volume (Å^3)	1507.9
Z	2
Density (calculated)	1.511 Mg m^{-3}
Absorption coefficient	1.016 mm^{-1}
F(000)	702
Crystal size (mm^3)	0.32 x 0.30 x 0.28
θ range for data collection (^{0})	2.19 to 34.72
Limiting indices	$-15 \le h \le 14$, $-21 \le k \le 18$, $-18 \le l \le 18$
Reflections collected	33127
Independent reflections	9621 [R(int) = 0.0354]
Completeness to θ = 34.72	73.9 %
Absorption correction	None
Refinement method	Full-matrix least-squares on F^2
Data / restraints / parameters	9621/0/388
Goodness-of-fit on F^2	1.123
Final R indices [$I > 2\sigma(I)$]	R1 = 0.0586, wR2 = 0.1427
R indices (all data)	R1 = 0.1148, wR2 = 0.1624
Largest diff. peak and hole (e Å^{-3})	0.687 and –0.503

Table 2 Selected bond length (Å) and bond angles (°) of complex **4**

Bond lengths (Å)		Bond angles (°)	
Cu(1)–O(5)	1.879(2)	O(5)–Cu(1)–N(1)	92.07(11)
Cu(1)–N(1)	1.984(3)	O(5)–Cu(1)–N(3)	89.83(11)
Cu(1)–N(3)	1.999(3)	N(1)–Cu(1)–N(3)	161.79(11)
Cu(1)–N(2)	2.015(3)	O(5)–Cu(1)–N(2)	163.64(11)
S(1)–C(13)	1.767(3)	N(1)–Cu(1)–N(2)	101.04(11)
S(1)–C(14)	1.769(3)	N(3)–Cu(1)–N(2)	80.78(11)
N(1)–C(7)	1.292(4)	C(7)–N(1)–Cu(1)	121.9(2)
N(1)–C(8)	1.426(4)	C(8)–N(1)–Cu(1)	120.7(2)
O(5)–C(4)	1.302(4)	C(4)–O(5)–Cu(1)	125.4(2)
N(3)–C(20)	1.328(5)	C(20)–N(3)–Cu(1)	126.1(2)
N(3)–C(24)	1.343(4)	C(24)–N(3)–Cu(1)	115.0(2)
N(2)–C(31)	1.328(4)	C(31)–N(2)–Cu(1)	127.8(2)
N(2)–C(26)	1.348(4)	C(26)–N(2)–Cu(1)	114.3(2)

Table 3 Binding constant (K_b), quenching constant (K_{sv}) and apparent binding constant (K_{app}) values between DNA and complexes **1**–**4**.

Compound	K_b (M^{-1})	K_{sq} (M^{-1})	K_{app} (M^{-1})
1	0.652×10^4	0.31×10^5	0.40×10^6
2	0.917×10^4	1.70×10^5	1.60×10^6
3	0.892×10^4	0.43×10^5	0.56×10^6
4	0.902×10^4	1.03×10^5	0.91×10^6

Table 4 Electrochemical parameters for the interaction of DNA with copper complexes

Complexes	[a]ΔEp (V)		[b]$E_{1/2}$ (V)		I_{pa}/I_{pc}	K_+/K_{2+}
	Free	Bound	Free	Bound		
1	0.279	0.302	0.140	0.132	1.15	0.951
2	0.128	0.145	–0.060	–0.058	0.92	1.168
3	0.129	0.134	–0.054	–0.048	0.97	0.836
4	0.155	0.178	–0.128	–0.115	0.95	0.985

[a]$\Delta Ep = Ep_a - Ep_c$; [b]$E_{1/2}$ is calculated as the average of anodic (Ep_a) and cathodic (Ep_c) peak potentials. [b]$E_{1/2} = Ep_a + Ep_c/2$.

Table 5 The calculated E-total value of binding of the copper(II) complexes with DNA (423D)

Complex	E-Total Value[a] (kcal mol^{-1}) (PDB ID: 423D)	Inhibitory constant (μM)	Binding region
1	–4.62	407.44	GC–AT
2	–4.83	287.45	GC–GC
3	–4.32	602.07	GC–GC
4	–4.72	347.94	GC–AT

[a]Calculated by Autodock.

Table 6 Protein binding constant (K_b), quenching constant (K_q) and number of binding sites (n) of complexes **1**–**4**

Complex	K_b (M^{-1})	K_q (M^{-1})	n
1	7.53 x 10^3	1.20 x 10^5	0.94
2	1.14 x 10^4	1.22 x 10^5	0.95
3	2.06 x 10^4	1.88 x 10^5	1.07
4	5.63 x 10^3	1.02 x 10^5	0.92

Table 7 In vitro cytotoxicity studies of copper(II) complexes against A549 and Huh7 cell lines

	IC_{50}	
Compound	A549 (μM)	Huh7 (μM)
1	21.06	10.64
2	15.93	16.84
3	12.32	23.01
4	18.74	31.65
L	26.45	38.27

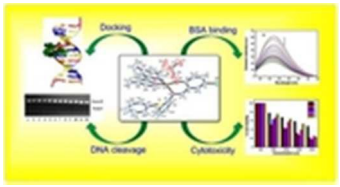

14x7mm (300 x 300 DPI)